CERN / DRDC 93-28
DRDC / P50
August 13th, 1993

R&D Proposal

Shashlik Calorimetry

A combined Shashlik + Preshower detector for LHC.

J. Badier, G. Bonneaud, A. Busata, Ph. Busson, C. Charlot, L. Dobrzynski[1], Ch. Gregory, A. Karar, R. Tanaka
Ecole Polytechnique, Palaiseau, FRANCE

Ph. Bloch[2], J. Christiansen, H. Heijne, M. Glaser, P. Jarron, F. Lemeilleur, I. Karyotakis[3], R. Loos, A. Marchioro, E. Rosso
CERN, Geneva, SWITZERLAND

A. Cheremukhin, A. Egorov, I. Golutvin, I. Ivanchenko, Y. Kretov, Y. Kozlov, V. Minashkin, P. Moissenz, A. Rashevsky, S. Sergueev, A. Sidorov, E. Zubarev, N. Zamiatin, A. Zarubin,
JINR, Dubna, RUSSIA

S. Abdullin, V. Kaftanov, V. Lukashin, A. Nikitenko, Y. Semenov, A. Starodumov, N. Stepanov, Y. Trebukhovsky
ITEP, RUSSIA

S. Bityukov, A. Gorin , V. Obraztsov, A. Ostankov, B. Polyakov, V. Rykalin, V. Soushkov, V. Vasil'chenko, A.Zaitchenko
IHEP, Protvino, RUSSIA

G. Atoyan, S. Gninenko, E. Guschin, V. Issakov, V. Klimenko, V. Marin, Y. Musienko, A. Poblaguev, V. Postoev , A. Proskurjakov, B. Semenov, I. Semenyuk, V. Sukhov
INR, Moscow RUSSIA

P. Bordalo, C. Lourenco, Ri. Nobrega, V. Popov[4], S. Ramos, J. Varela
LIP, Lisboa, PORTUGAL

E. Clayton, D. Miller, C. Seez, T.S. Virdee
Imperial College, London, UK

R.M. Brown, D.J.A. Cockerill, J. Connolly, L. Denton, R. Stephenson
Rutherford Appleton Laboratory, Didcot,UK

P.R. Hobson, D.C. Imrie
Brunel University,Uxbridge , UK

---

[1] Spokesperson
[2] Contact person
[3] on leave from LAPP, Annecy
[4] on leave from INR, Moscow

Abstract

New techniques have been developed to read out the light from lead/scintillator sampling calorimeters. These techniques involve the use of wavelength shifting optical fibres. The light yields from such calorimeters are in excess of 10000 photons per GeV. The use of optical fibres enables fine lateral segmentation to be achieved with a minimum of dead space. In addition, it is expected that such calorimeters can be built at a relatively low cost. The first results, from a non-projective calorimeter prototype exposed to high energy electrons, are encouraging. The measured energy resolution is:

$$\frac{\sigma}{E} = \frac{(8.4\pm.1)}{\sqrt{E}} \oplus \frac{(.37\pm.03)}{E} \oplus (.8\pm.2) \quad \% \quad (E \text{ in } GeV)$$

The angular resolution deduced from measurements is:

$$\sigma_\theta(\text{mrad}) = \frac{70}{\sqrt{E}}$$

Further research and development are essential before building a full scale projective detector. In this paper we present the current status of the Shashlik calorimeter and the program of research and development that we wish to undertake.

TABLE OF CONTENTS

1. Introduction

In order to search for new phenomena at the LHC good electromagnetic calorimetry will be essential. In the CMS detector we wish to achieve the following performance for the electromagnetic calorimeter:

- energy resolution at least as good as $\sigma/E=0.10/\sqrt{E}$ and a constant term of 1%,
- operation in the presence of high magnetic field[1];
- high radiation resistance[2];
- high speed[3];
- as good a hermeticity as possible.

The Shashlik detector has been designed to meet these requirements. It is a lead/scintillator sandwich calorimeter having the crucial properties of compactness, timing, good spatial resolution and low cost.

In the mid-1980's Fessler et al[4] suggested the use of WLS optical fibres for the readout of scintillation light from sandwich electromagnetic calorimeters. Four years later INR(Moscow) and IHEP(Protvino)[5] developed a process for mass production of scintillator tiles and lead plates with the holes necessary for the insertion of the WLS fibres.

The first beam-test measurement results for a prototype of the calorimeter performed at CERN4, BNL and IHEP5 showed that it was possible to:

- obtain good energy resolution and π/e separation,
- obtain good light collection and light transmission efficiency;
- obtain promising results with photo detectors which can work in high magnetic field (silicon photodiodes, tetrodes...),
- minimize dead space and thus obtain good lateral uniformity of response,
- build a compact calorimeter with a high degree of hermeticity;

2. The Shashlik calorimeter.

2.1. Description.

The design of an individual CMS prototype module developed by the Ecole Polytechnique-INR-IHEP collaboration is shown in Figure 1. Each module is a 47 x 47 x 440 mm^3 lead/scintillator sandwich, made out of perforated lead (2.0±0.005 mm) and plastic scintillator(4±0.05 mm) plates. Altogether, there are 75 layers giving a total radiation length of about 27.5 X_0 .

[1] up to 4 Tesla
[2] >1 Mrad/year
[3] 25 nsec bunch crossing
[4] H. Fessler et al., Nucl. Instr. and Meth. 228(1985)303.
[5] G. S. Atoyan et al. Nucl. Instr. and Meth. (to be published),,Preprint INR-736/91, INR, Moscow (1991)

Each plate of the module has 25 holes in it, arranged as a 5 x 5 square matrix. WLS fibres were inserted into these holes perpendicularly to the plates. The fibre ends were collected in one bunch, polished, and were viewed directly by a photomultiplier tube and/or a Si photodiode. The total number of fibres was 13 (12 with loops + 1 single) in the version readout by photomultiplier[6] and 25 in the version readout by Si photodiode (for details see table 1). In this last version Kuraray Y7 WLS fibres were used. These were aluminized[7] at the front face of the towers.

The scintillator plates were manufactured at IHEP with casting technology[8]. This produces plates with a surface of high optical quality including the surface of the holes for fibres. Perforated lead plates, containing 5% antimony additive to increase their rigidity, were manufactured by cold punching. White paper (20 mg/cm, 0.1 mm thick) was placed between the lead and scintillator plates to act as a reflecting surface. The paper was perforated by the same punch as the lead plates. The module as a whole was wrapped with aluminized mylar and held together by 4 bicycle rods fixed to aluminum plates at the front and at the rear of each tower. The composition and properties of the sampling layers are summarized in table 1 for the CMS[9] prototype.

Tower lateral size	47 x 47 mm^2
Number of planes	75
Total depth (465 mm	27.5 X_0
Mean radiation length (X_0)	16.9 mm
Moliere radius	34 mm
Lead thickness	2 ± .005 mm
Scintillator type[10]	Polystyrene + .5% POPOP + 2% Para-Terphenyl
Scintillator thickness	4 ±.05 mm
Type of WLS fibres[11]	Y7
Number of fibres	25
Fibre diameter	1.2 ±.03 mm
Hole diameter in scintillator	1.3 mm
Hole diameter in lead	1.5 mm

Table 1: Main parameters of CMS prototype Shashlik tower.

The optimal number of WLS fibres in the module was chosen, on the one hand, by

[6] In this version we used K27 WLS fibres produced at INR.
[7] The aluminization was done by Precitrame S. A. CH2720 TRAMELAN.
[8] V.K.Semenov et al., Preprint JINR 13-90-16, Dubna (1990) (in Russian).
[9] J. Badier et al., Preprint CMS TN / 93-66, INR - 821/93, X-LPNHE / 93-4.
[10] This scintillator was produced in Russia.
[11] The Y7 WLS fibres are produced by Kuraray. We have also used K27 WLS fibres produced at INR(Moscow).

the requirement of maximum light collection with minimum lateral non uniformity (corresponding to a less than 2% contribution to energy resolution) and, on the other hand, by cost and technological considerations.

A more precise estimate of the optimal number of fibres was obtained by Monte Carlo calculation of the light collection non uniformity. The efficiency with which the light is captured by an individual fibre is well described by the model of L. Labarga and E. Ros[12].

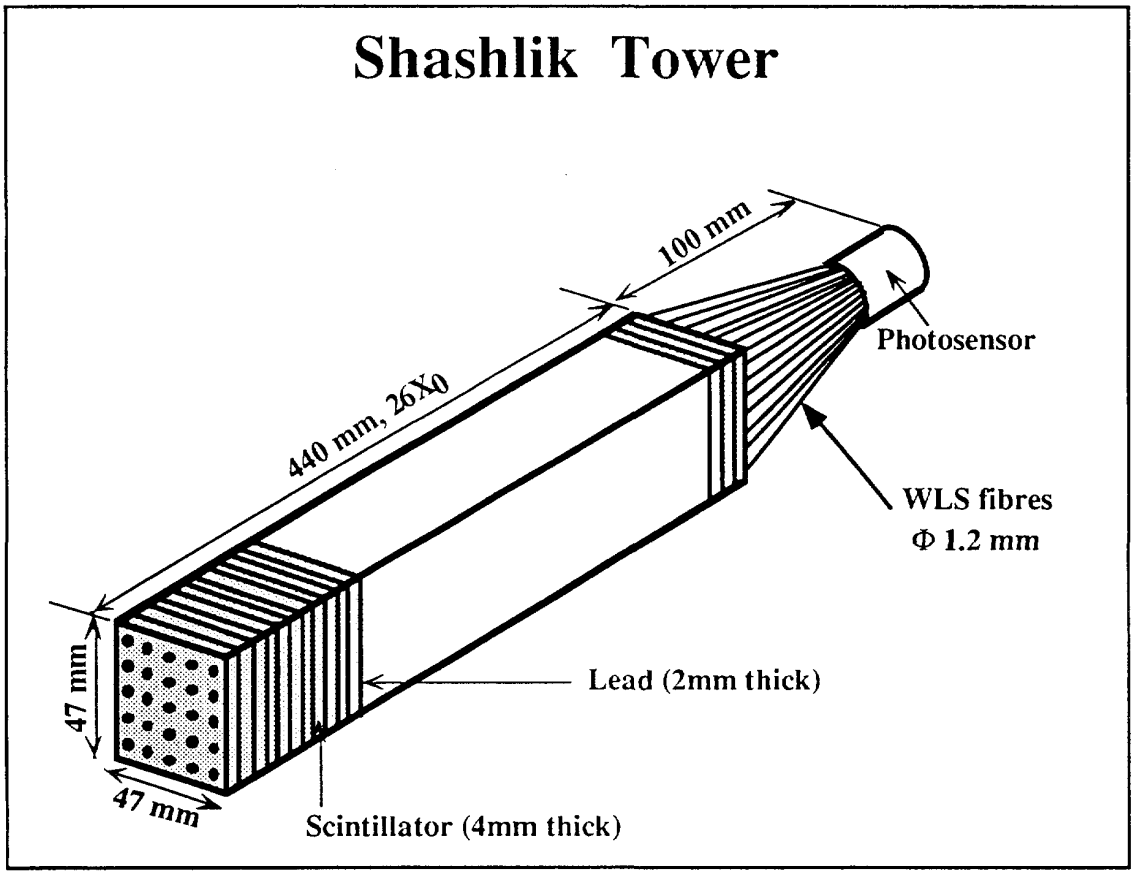

Figure 1. Mechanical design of a CMS Shashlik calorimeter prototype tower equipped with 25 aluminized WLS fibres.

The WLS fibres are required to have a light attenuation length of at least 1.5 m, when used in Shashlik towers with a length of 40 cm. This limits contributions to the "constant term" of the energy resolution function, due to longitudinal fluctuations of the electromagnetic shower, to about 1%.

The WLS fibres are required to have good optical uniformity and long-term mechanical stability. Non uniformity in the optical properties of the fibres can lead to a decrease in the light

[12] Labarga and E.Ros, Preprint Univer. Siegen, FTUAM-EP-86-3,(1986).

yield[13]. There is also an additional contribution to the energy resolution of the order $\sigma/\sqrt{N}$, where σ is the dispersion of fibre to fibre response and N is the number of fibres which contribute to the total light yield from an electromagnetic shower[14]. The diameter dispersion of the fibres should not exceed ±0.03 mm. This is important when the calorimeter modules are assembled mechanically and fibres are inserted into the holes.

The first WLS fibres used for the prototypes were "Polychrome-26" fibres developed and produced at INR (Moscow). The core of this optical fibre is made of polystyrene with a refractive index of n =1.59. The cladding is made of fluorinated PMMA with n =1.40. The core contains luminophor with the absorption spectrum λ_{max} =450 nm, which matches quite well the emission spectrum of the Pterphenyl+POPOP scintillator. The luminophor emission spectrum has λ_{max}=530nm.

The WLS fibres were fed through the entire length of the tower, looped around at the front of the tower and fed back through the tower to complete the insertion process. The photomultiplier then sees both ends of the same fibre at once. Such a loop acts as an almost ideal mirror with the reflection coefficient > 95%[15]. The effective light absorption length in the fibres of the module was ~ 1.2 m. Looping the fibres avoids the necessity of aluminizing the fibres ends at the front of the tower. This could lead to a greater uniformity of light collection.

In the CMS modules we tested in the beam, we used K27 WLS fibres with the loops and Kuraray Y7 fibres cut at the front of the tower and aluminized. The two methods gave us about the same light yield.

[13] For example this is due to the large number of reflections for individual photon (a simple optical simulation gives about 250 for our case).

[14] From the same simulation, one has N ~ 150 in our case for 1 GeV

[15] for a loop with the radius 3 cm the light losses are < 5%

3. Measured performance of the CMS Shashlik prototypes.

The nine parallelipedical Shashlik towers assembled in a 3 x 3 matrix (figure 3) were tested in October 1992 at the CERN SPS. The amount of material in front of the first scintillator tile was the equivalent of a standard lead plate.

The WLS fibres (Y7) were cut at the front of the tower and aluminized[16]. The fibres were bunched together at the rear of the tower and cut with a diamond mill. A hexagonal Plexiglas light mixer was used to couple[17] the fibres to a Silicon photodiode[18]. Each photodiode was followed by a preamplifier whose characteristics are given in reference 9. Figure 2 gives the observed signal at the preamplifier output and its main parameters.

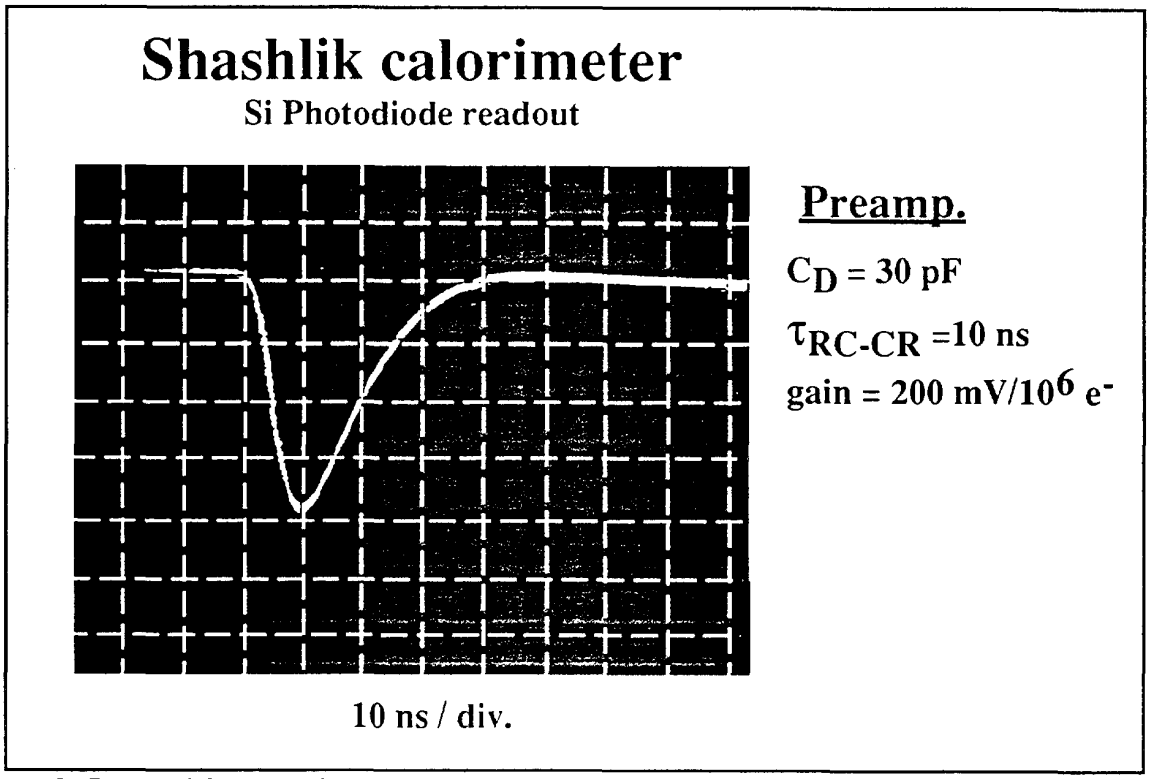

Figure 2: Preamplifier signal output.

The calorimeter was mounted on a platform which could be moved horizontally and vertically with respect to the beam line with a precision better than 0.1 mm. The detector could also be rotated around its vertical axis, so that the particles could be sent into the detector at an angle θ_z (usually a few degrees in the horizontal plane) with respect to the fibres axis.

[16] The aluminization was done by Precitrame S. A. CH2720 TRAMELAN.
In a previous test reported in CMS TN/ 92-45, we used K27 WLS fibres produced at INR (Moscow). Twelve fibres were bent at the front of the module and one single fibre was running through the hole situated at the center of the tower.

[17] The towers were also readout by Russian photo multipliers during the September 92 test(see CMS TN/ 92-45).

[18] We used 10 x 10 mm^2 HAMAMATSU photodiodes.

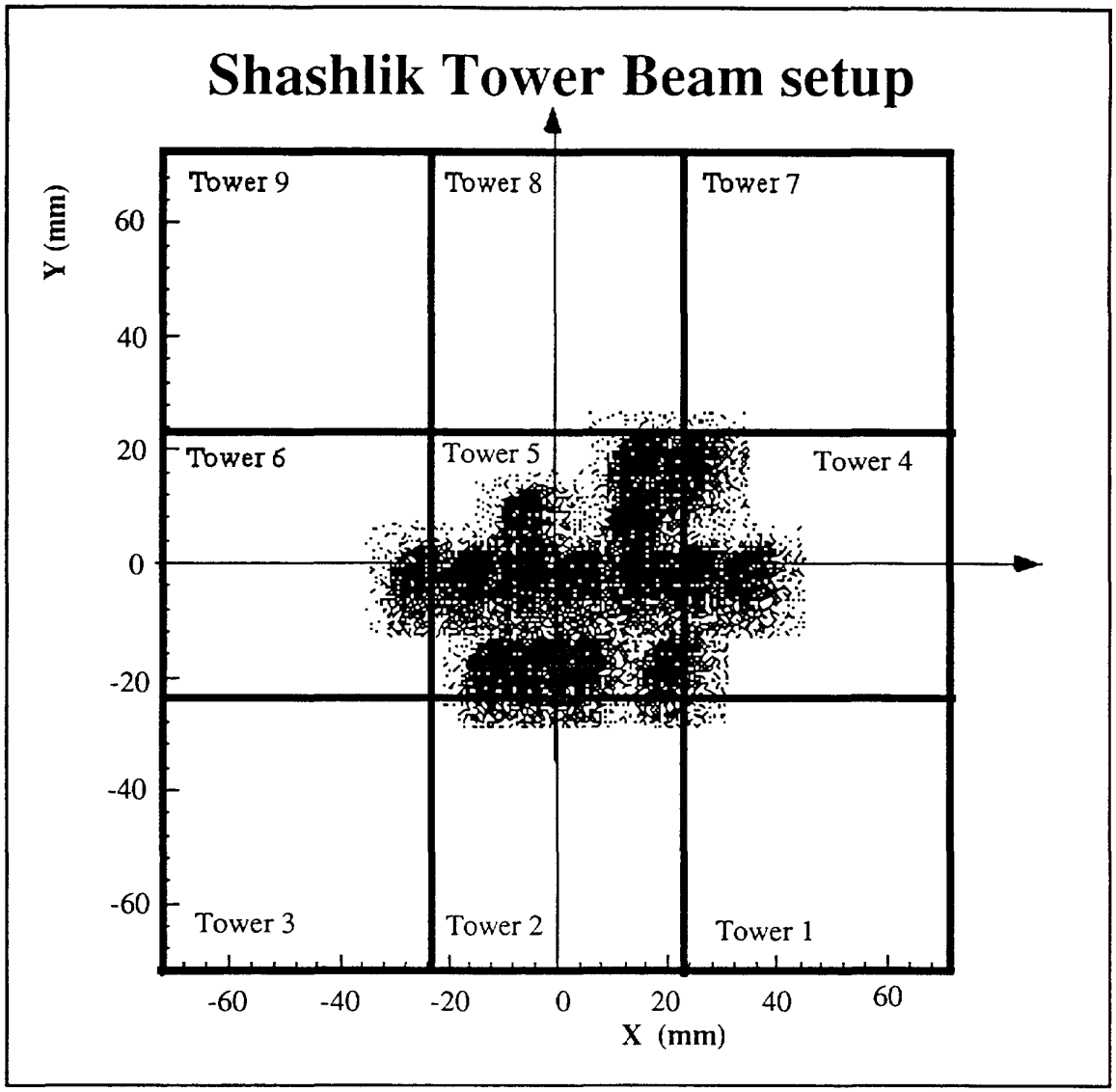

Figure 3 Shashlik nine tower calorimeter setup. The black points correspond to electrons hitting the calorimeter.

Upstream of the calorimeter, a trigger counter telescope was installed. It consisted of five scintillation counters (S_1 - S_5). Two drift chambers (U_1, U_2) with x, y readout situated at 5 m from each other were used to define the beam impact point into the calorimeter.

Negative particle beams of 10, 20, 40, 80, and 150 GeV were sent into the detector at θ_z=0° respect to the fibre axis. The beam particle rates were 10^2 - 10^3 events per spill. At high energies (≥ 40 GeV), the contamination of pions in the electron beam was small and in the analysis presented here no attempt was made to eliminate an eventual pion contamination.

The towers were calibrated with 40 GeV electrons. About 3000 electrons were sent into the central region of each tower at normal incidence. On average ≈85% of the electromagnetic shower energy was deposited in the tower under calibration. The calibration constants were estimated with a statistical precision of 0.2% from these data. For the analysis presented here, all measurements were corrected with the calibration constants.

The results described here were obtained by analyzing the following sets of data taken at normal incidence(θ_z=0°).

• *Electrons of 10, 20, 40, 80 and 150 GeV entering the central region of the central tower of the nonet* were used to establish the energy resolution.

• *Electrons of 40 GeV hitting the central tower of the nonet (figure 3)* have been taken and used for the study of the uniformity response of the calorimeter. The beam size was 20 x 20 mm^2 and data have been taken for beam position hitting tower 5 at distances of 10 mm from each other.

• *Electrons of 10, 20, 40, 80 and 150 GeV entering the central region of tower 5 preceded by a 2.5 cm thick lead plate* are used to study ability to reconstruct the shower position when a preshower detector is placed at ~4.5 X_0 The angular resolution of the shower direction is obtained from the reconstructed position of the shower in the active part of the calorimeter and the assumed position in a preshower detector.

3.1. The uniformity of the calorimeter response.

For all the electron data taken in tower 5 (figure 3) we have displayed in figure 4 the normalized difference of the measured energy and the mean energy as function of the X and Y electron impact coordinate. One sees a dispersion of about ±3 %, for the raw data. In figure 4a one sees that at the left edge of the tower the energy is as high as at the center. One possible explanation of this effect could be a higher reflectivity of the light at this edge compared to the other tower edges. Compared to the response at the center of the tower the measured energy is lower by 3-4 % at the other edges of the tower. This is due to the non containment

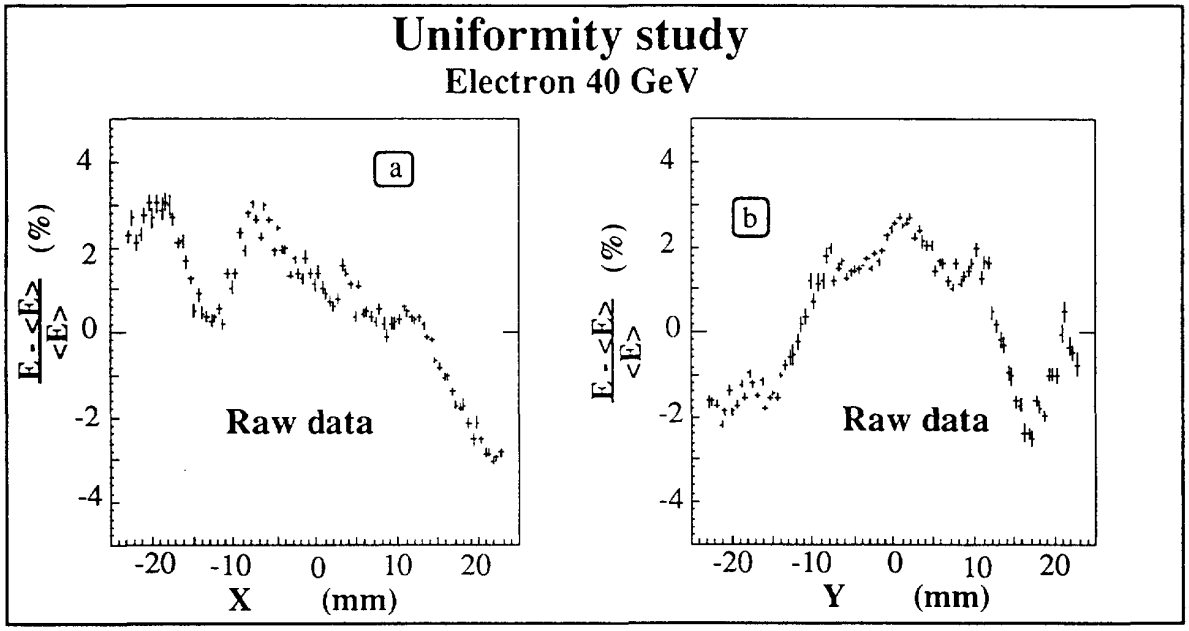

Figure 4: Tower 5 uniformity response for raw data.

of the shower near to the tower edges.

When one applies the energy corrections defined in reference 9, the same data are shown in figure 5.

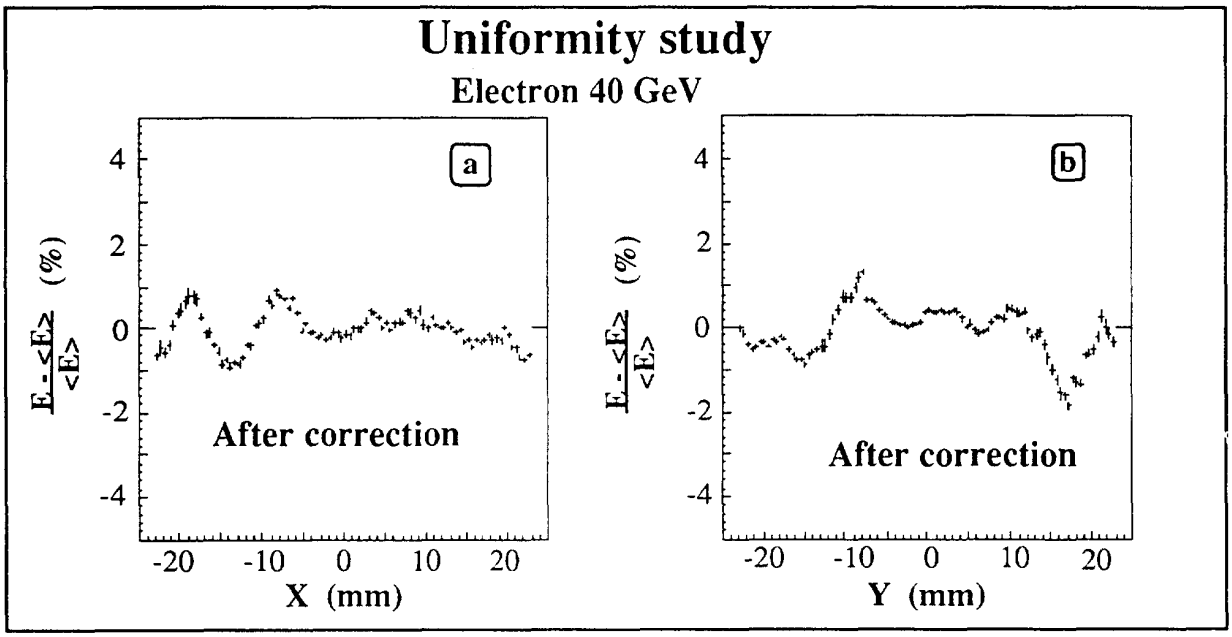

Figure 5: Tower 5 uniformity response for corrected data.

Figure 6 shows the projections of figures 5a and 5b on the vertical axis. The curves are gaussian fits to the data. One sees that the energy dispersions have respectively a σ = 0.4 % and 0.3% for X and Y beam profiles.

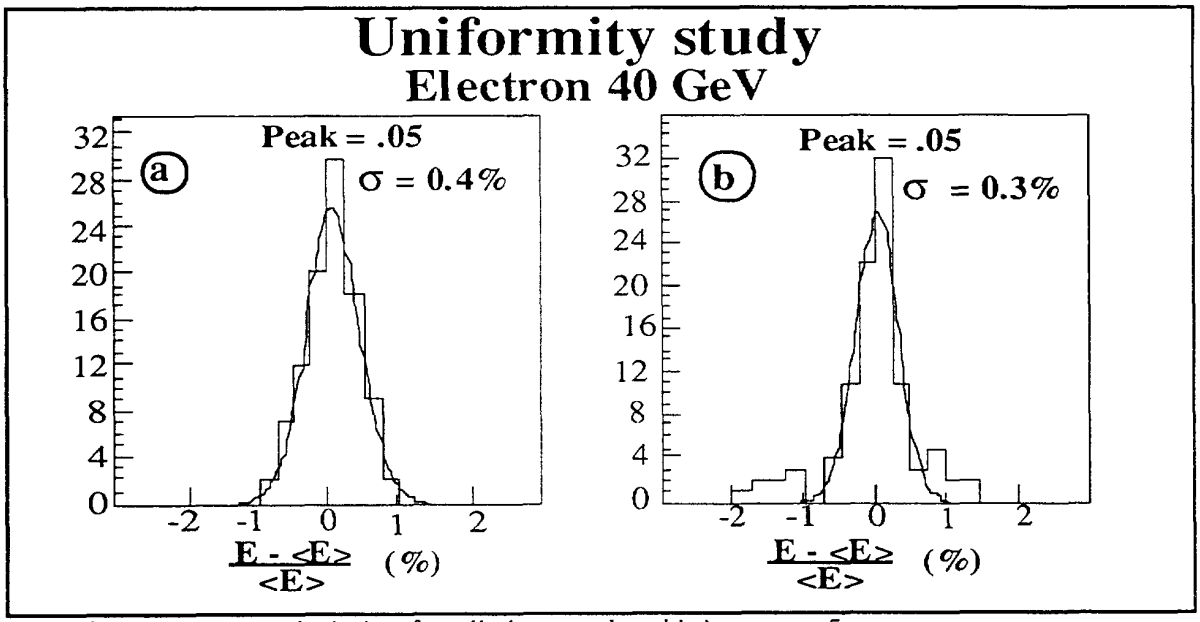

Figure 6: Mean energy deviation for all electron data hitting tower 5:
a) for X projection (fig. 5a) and b) for Y projection (fig. 5b)

After corrections the non-uniformities[19] are generally less than ±1%, with the σ of the dispersions being much smaller (0.4%).

3.2. Energy resolution of the Shashlik calorimeter.

The energy resolution at various energies has been extracted using Gaussian fits and is shown in figure 7. We have fitted the measured points to :

$$\frac{\sigma}{E} = \frac{a}{\sqrt{E}} \oplus \frac{b}{E} \oplus c$$

where:

- a represents the contribution of the sampling fluctuations,
- b the electronic noise term,
- and c the constant term contribution

to the energy resolution.

The result of the fit is given in table 2 for different types of readout.

Readout	Best Fit
Si Photodiodes	$\frac{\sigma}{E}(\%) = \frac{(8.4\pm.1)}{\sqrt{E}} \oplus \frac{(.37\pm.03)}{E} \oplus (.8\pm.2)$
PM + 1 Si photodiode on tower 5 (central)	$\frac{\sigma}{E}(\%) = \frac{(8.4\pm.6)}{\sqrt{E}} \oplus \frac{(.08\pm.01)}{E} \oplus (.9\pm.1)$
PM	$\frac{\sigma}{E}(\%) = \frac{(9.0\pm.1)}{\sqrt{E}} \oplus (1.0\pm.3)$

Table 2: Shashlik energy resolutions for various used readout.

One sees that the sampling term achieved with a Si photodiode readout is 8.4%. The electronic noise term for a single diode[20] was measured to be 84±6 MeV. Its contribution to the energy resolution, for all 9 towers readout with Si photodiodes is 371 ± 27 MeV. This value is somewhat larger than the extrapolation from the single photodiode measurement, probably due to contributions from correlated noise. A new preamplifier is under study and will be tested in our next test-beam period. We will take special care to minimize the correlated electronic noise.

The constant term which comes out of the fits is always smaller than 1%[21].

[19] The regions around the fibres(r = 1 mm) and the region near the edges of the tower (0.5 mm) are excluded.
[20] The Si photodiode was mounted on the central tower of the nonet.
[21] (.8 ± .2)%

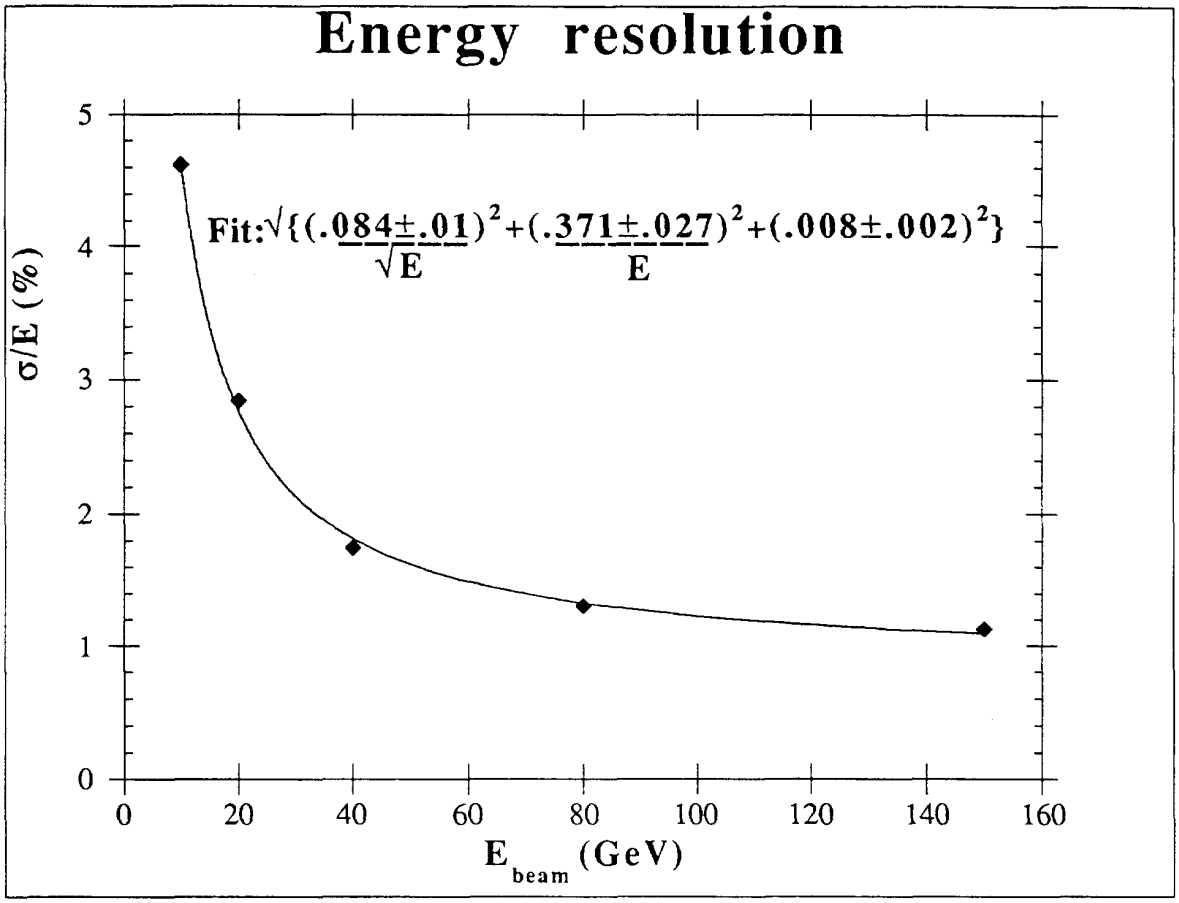

Figure 7: Shashlik energy resolution measurement.

3.3. Shower position measurement.

The shower center is estimated from the lateral energy distribution by the following asymmetry variable[22]:

$$A(x) = \frac{\sum_{i<imax} E_i - \sum_{i>imax} E_i}{E_{tot}}$$

where i_{max} denotes the interval in which the deposited energy is maximum. The details of this study are described in reference 23. The precision of the reconstructed shower center is deduced from the asymmetry measurement by:

$$\delta x = \frac{1}{\left|\frac{dA}{dx}\right|} \sigma_A$$

[22] J. Badier et al., Preprint CMS TN / 93-65, INR - 823/93, X-LPNHE / 93-3.

For 40 GeV electron data we show in figure 8 the variation of error on the shower position as a function of the electron impact point.

The precision in the shower position has been measured **at the tower center** as a function of the energy. The best fit to the data is obtained with a quadratic form of type:

$$\sigma_{x,y}(mm) = \frac{9.1 \pm 0.3_{stat} \pm 0.7_{syst}}{\sqrt{E}} \oplus \frac{27 \pm 1.4_{stat} \pm 2.1_{syst.}}{E}$$

The precision on the shower position is worst at the tower center. Towards the tower edges it is better by a factor of 3.

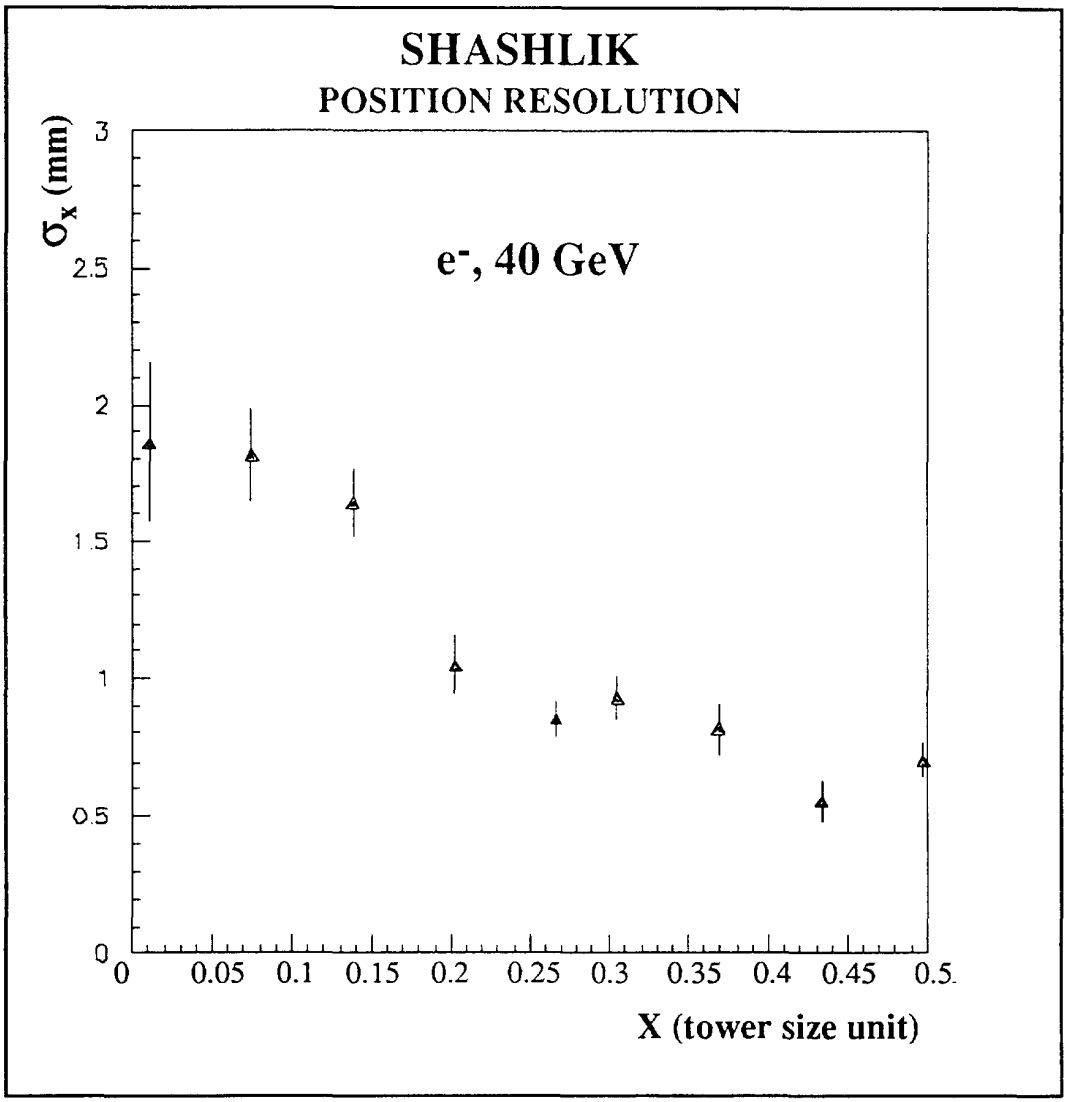

Figure 8: Precision of the reconstructed shower position for 40 GeV electrons hitting tower 5 of our setup.

3.4. Shower angular resolution.

To achieve the measurement of the direction of a shower, one needs to have two independent position measurements. We assume that one position is given by the shower barycentre in the Shashlik and the other by a preshower detector placed at about 3 X_0. To estimate the resolution on the shower direction, we have exposed the Shashlik calorimeter to electrons with ~5 X_0 lead in front of it. From these measurements, it is possible to get the error on the electron shower direction. The variation of σ_θ as function of the electron incident energy is given in figure 9. This prediction (extrapolated from the data) was obtained by assuming a precise position at a depth of 3 X_0. For this estimation we used the average longitudinal shower maximum position of $\langle m \rangle = 6.0 + 1.0 \, Ln \, E$ (in radiation lengths).

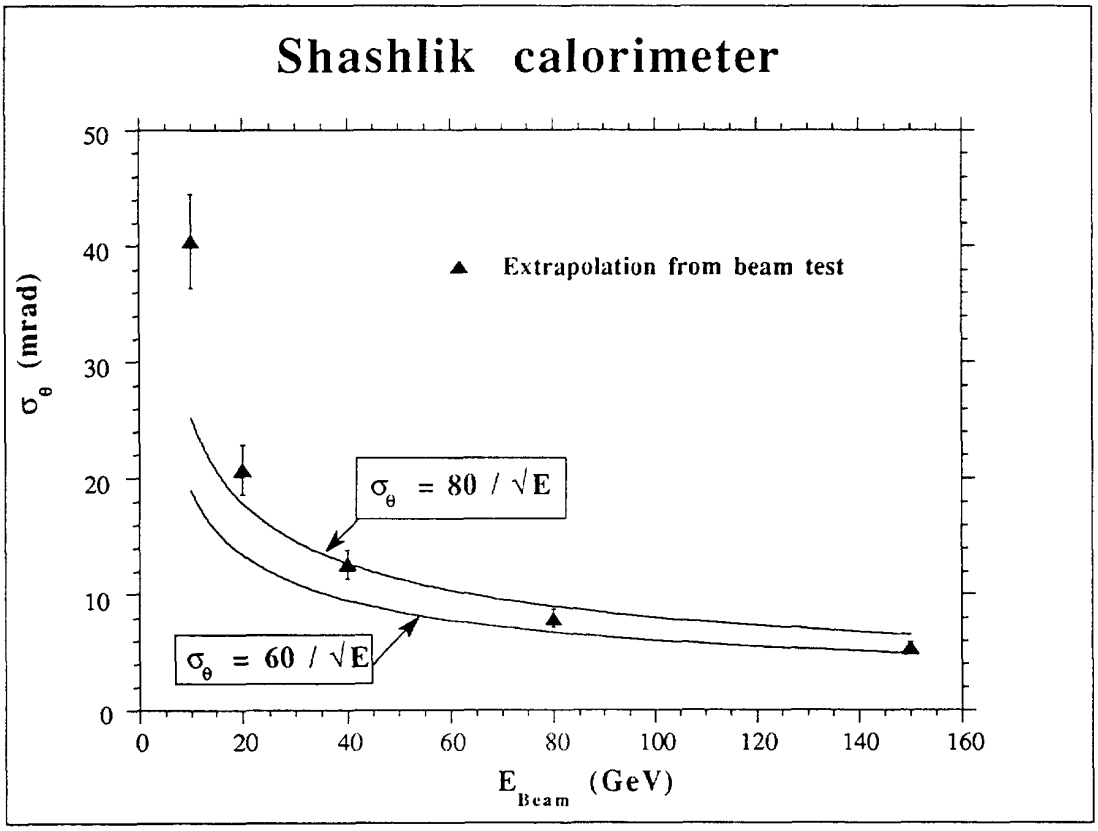

Figure 9: Angular resolution. of the reconstructed shower direction when a preshower detector is placed at 3 X_0 in front of the Shashlik Calorimeter.

One sees that with a preshower detector coupled to a Shashlik calorimeter one should obtain an angular resolution of:

$$\sigma_\theta(mrad) = \frac{70}{\sqrt{E}} \qquad (E \geq 40GeV)$$

at the tower center. Averaging over the tower should lead to an improvement of ~30%.

3.5. Light yield of a Shashlik tower.

The light yield provided by a Shashlik tower was measured with a Si photodiode connected to a low-noise charge-sensitive amplifier. The gain of the amplifier was measured by injecting a test charge through a calibration capacitance. Our estimation of the systematic error in these measurements is ±10%.

The light yield was measured in different experimental conditions. In the first measurement (September 1992) the central tower of our setup was equipped with 13 K-27 fibres out of which 12 had loops. The light yield provided by a 40 GeV electron shower hitting the center of the tower gives a signal equal to 292000 electrons (7300 electrons/GeV). 86% of the energy is deposited in the central tower. Using a quantum efficiency of 65% for the HAMAMATSU photodiode in the region of K-27 emission spectrum (λ = 525 nm), one estimates that the total observed light yield is ~13,060 γ/GeV.

In the second test period, the towers were equipped with 25 Y-7 KURARAY WLS fibres aluminized at the front end of the tower. The light yield measurements were performed this time on seven towers. The photodiode efficiency for Y-7 emission spectrum (λ = 500 nm) is 62.5% . For the central tower of the nonet we obtained 6400 electrons/GeV. A mean value of 6600 electrons/GeV was measured for the seven towers corresponding to 12,300 γ/GeV.

4. Test beam results[23] of a preshower detector with silicon strips.

4.1. Introduction.

In order to measure the direction of the electromagnetic shower and provide good π^0 rejection a preshower detector will be required at CMS. The preshower detector will provide shower coordinate information at the expense of a relatively small worsening of the energy resolution. After the preshower the shower is sampled by 2 mm pitch silicon strip detectors. The optimized solution in terms of cost, accuracy and number of layers is to have two layers of silicon detectors placed after $2X_0$ and $3X_0$ of absorber[24].

The analog signals from the strip detectors of the preshower are used to find the barycentre of the shower and to correct for the energy lost in the preshower absorber material.

4.2. Test beam setup.

The schematic of the beam test set-up is shown in figure 10.

Figure 10: Preshower test beam setup.

[23] Beam-test results of a preshower with Si strip detectors as active media. M. Glaser, et al., Submitted to the 1st International conference on Large Scale Applications and Radiation Hardness of Semiconductor Detectors. Floreze, Italy July 1993. Proceedings to be published in " Nuovo Cimento".

[24] see RD3.

Copper was used as the absorber material. Two silicon detectors (60 x 60 x 0.4 mm^3) with strips at a pitch of 2 mm were used (each one with 29 strips and guard ring along its perimeter). These detectors (figure 11) were manufactured by ELMA (Moscow) from 3.6 kΩcm n-type FZ-Wacker silicon material.

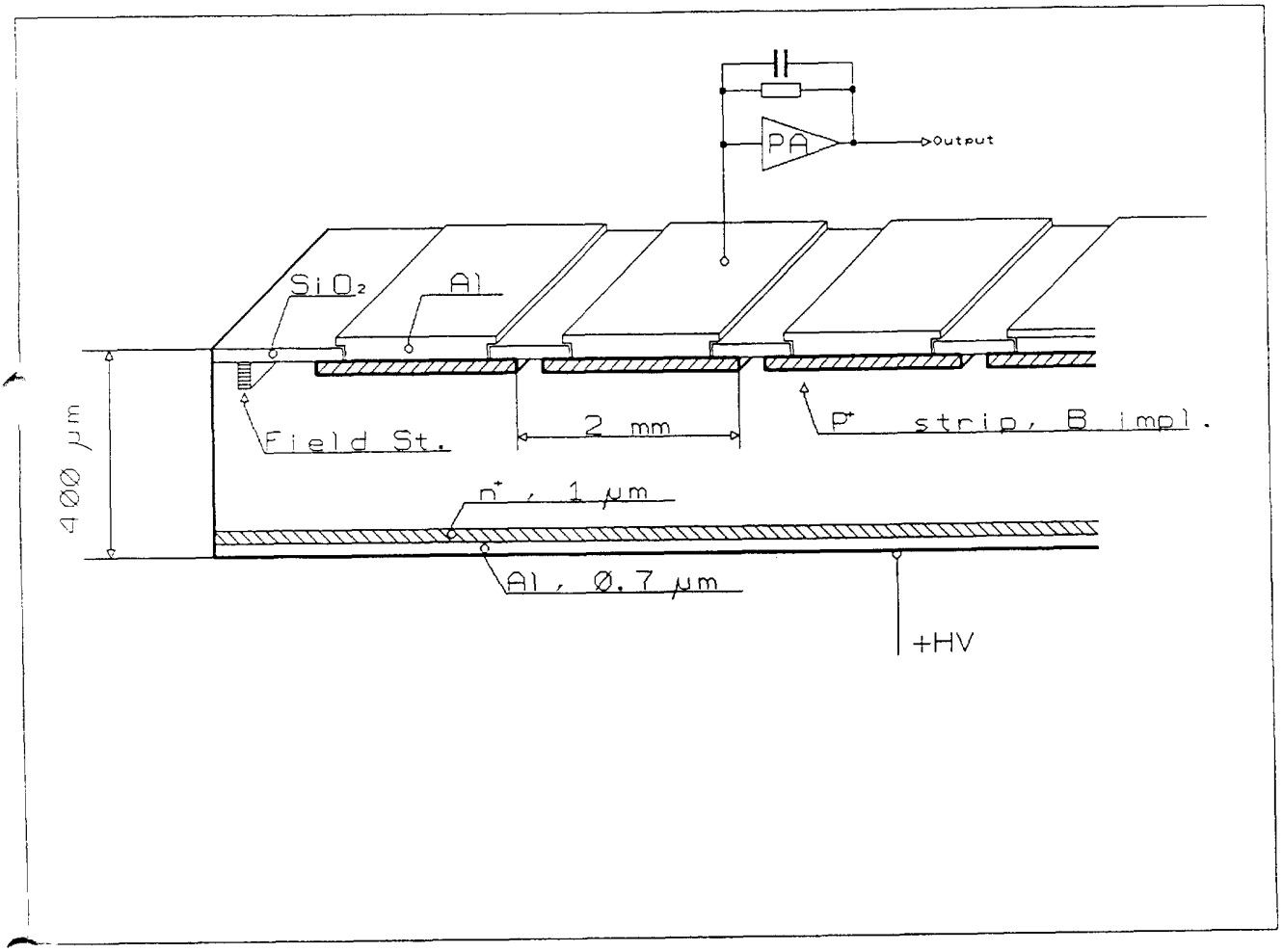

Figure 11: Preshower silicon strip detector.

Full depletion occurs at 170 V and each detector strip has a capacitance about 27 pF/cm^2. Each strip has an area of 1.2 cm^2 and a reverse current of about 50 nA (at 170V).

4.3. The readout.

A 16-channel AMPLEX-SICAL signal processor[25] was used to readout the silicon detector. Each detectors was connected to a printed board circuit containing two AMPLEX's (32 channels per board) as shown on figure 12.

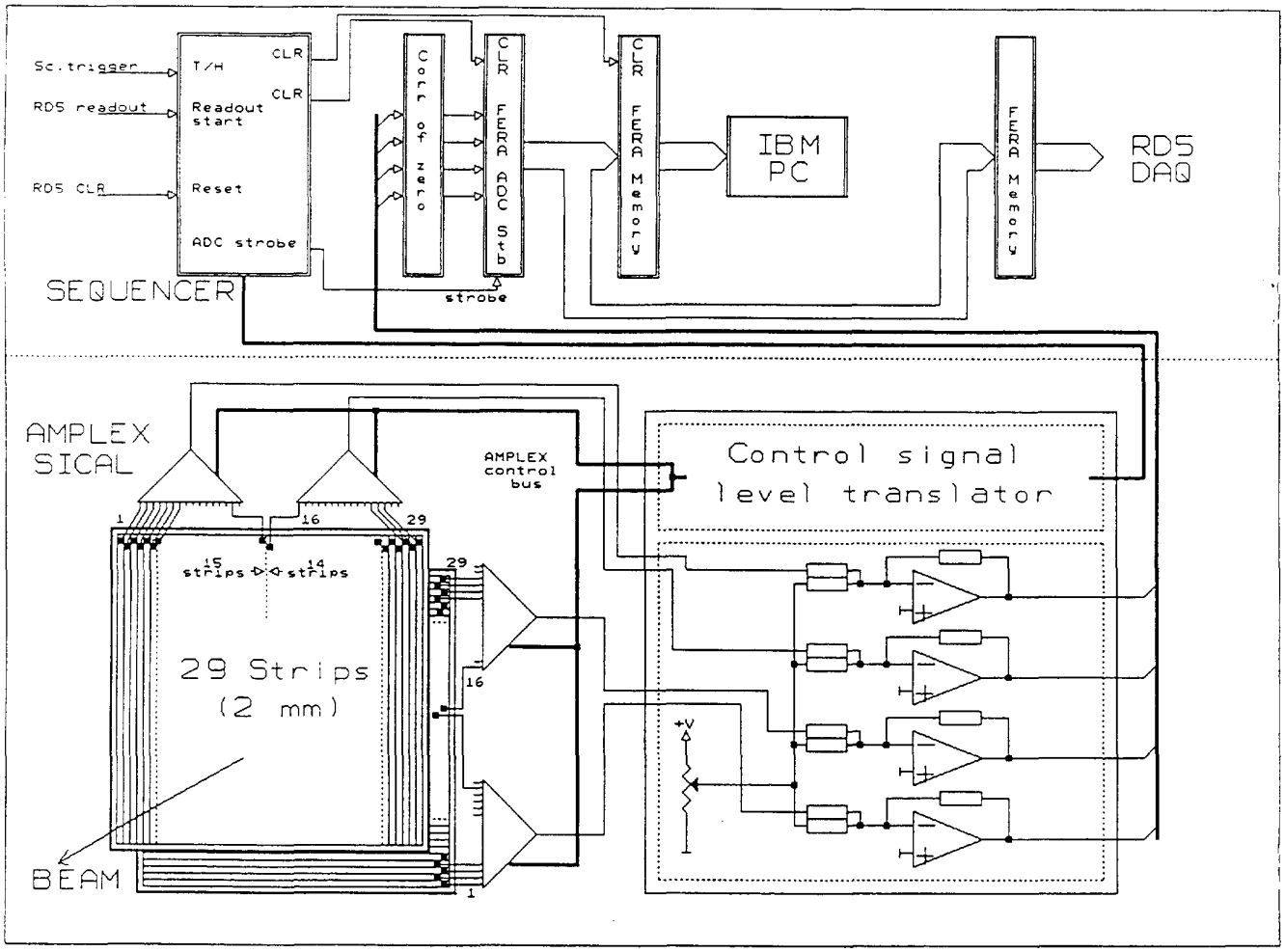

Figure 12 Preshower readout system.

The Si detectors were tested using a Am^{241} (5.5 MeV) alpha-source. The pulse height distribution from the alpha particles was obtained in a self triggering mode by "FAST-OR" signal from a single AMPLEX channel.

[25] E. Beuville at All., Nuclear Physics B. (Proc. Suppl.) 23A (1991) 198

4.4. Electron signals.

Figure 13 shows the total energy deposition in both silicon layers by 40 GeV electron showers.

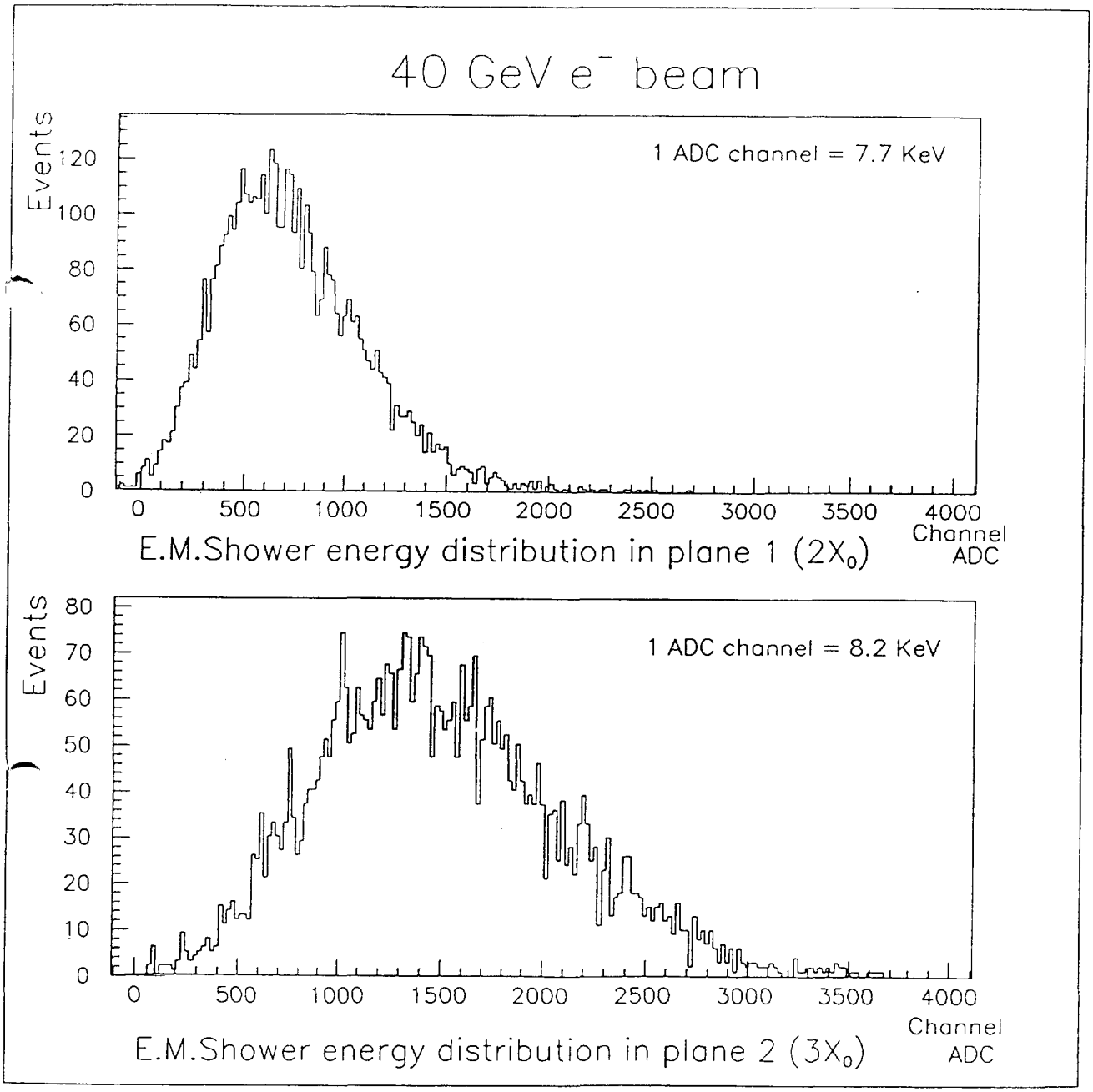

Figure 13: Shower energy loss in silicon planes 1 and 2.

4.5. Effect on the calorimeter resolution.

Data have been taken with and without the preshower in front of the calorimeter. A preliminary analysis (not shown) indicates that, using the energy deposited in the Si strips, the energy resolution is degraded by less than 10% in comparison to that obtained for the stand alone calorimeter.

4.6. Shower position resolution.

The analysis of coordinate reconstruction is under way. The Monte Carlo simulation indicates that a position resolution of .35 mm at 40 GeV should be achieved with 2 mm pitch strips placed after 3 X_0. Preliminary measurements (not shown) give results that are in agreement with our simulation.

5. Physics performance of a Shashlik+Preshower detector.

The benchmark for an electromagnetic calorimeter at LHC is the detection, at high luminosity, of an intermediate mass Higgs boson by way of its two photon decay. In the Standard Model there is an important mass range ($90 < m_H < 130$ GeV) in which only this channel is detectable. In the Minimal Super symmetric extension to the Standard Model this channel allows a direct search in a large fraction of the $\tan\beta$-m_A parameter space.

To perform well in detecting the Higgs two photon decay the electromagnetic calorimeter needs excellent energy resolution and good rapidity coverage. Efficient rejection of neutral pions and the measurement of the angle of incidence of the photon in the r-z plane ("photon pointing") are also required[26].

Table 3 shows the contributions to the width of a 100 GeV Higgs using the design parameters of the CMS Shashlik ECAL. The contributions are expressed as "effective R.M.S." calculated as half the width needed to contain 68.3% of the distribution. This variable provides a more reliable and relevant measure of the non-Gaussian distributions (such as the angular error, and the pile-up noise) than the width of Gaussian fits. It can be seen that the limiting factors on the two photon mass resolution, and hence the signal significance, are the stochastic and constant terms of the energy resolution, and the angular resolution. Charged tracks associated with the Higgs may be used to obtain a better estimate of the vertex position and hence reduce the error due to the angular resolution. The gain is most substantial at low luminosity, but it seems that some gain can be obtained even at high luminosity[27].

	CMS design goal	$\Delta m_{\gamma\gamma}$
$\Delta E/E$: Stochastic term	$9\%/\sqrt{E}$ (GeV)	760 MeV
Constant term	1%	680 MeV
Noise	300/E (MeV)	310 MeV
Angular resolution	70 mrad/$\sqrt{E}$ (GeV)	700 MeV
Pile-up noise (10^{34} cm^{-2}s^{-1})	use 12x12 cm^2	350 MeV
	TOTAL:	**1325 MeV**

Table 3: Contributions to the observed width of a 100 GeV Higgs.

Figure 14 shows the statistical significance, as a function of m_H, that would be obtainable in CMS after an integrated luminosity of 10^5 pb^{-1}, taken at 10^{34}cm^{-2}s^{-1}, using a Shashlik calorimeter covering $|\eta|<2.5$ with a barrel radius of 1.4m and the performance parameters given in table 3.

[26] C. Seez *et al*, Proc. Large Hadron Collider Workshop, Aachen, 1990, eds. G. Jarlskog and D. Rein, CERN 90–10, vol. III, 474
[27] C. Seez and T. S. Virdee, CMS TN/93-92

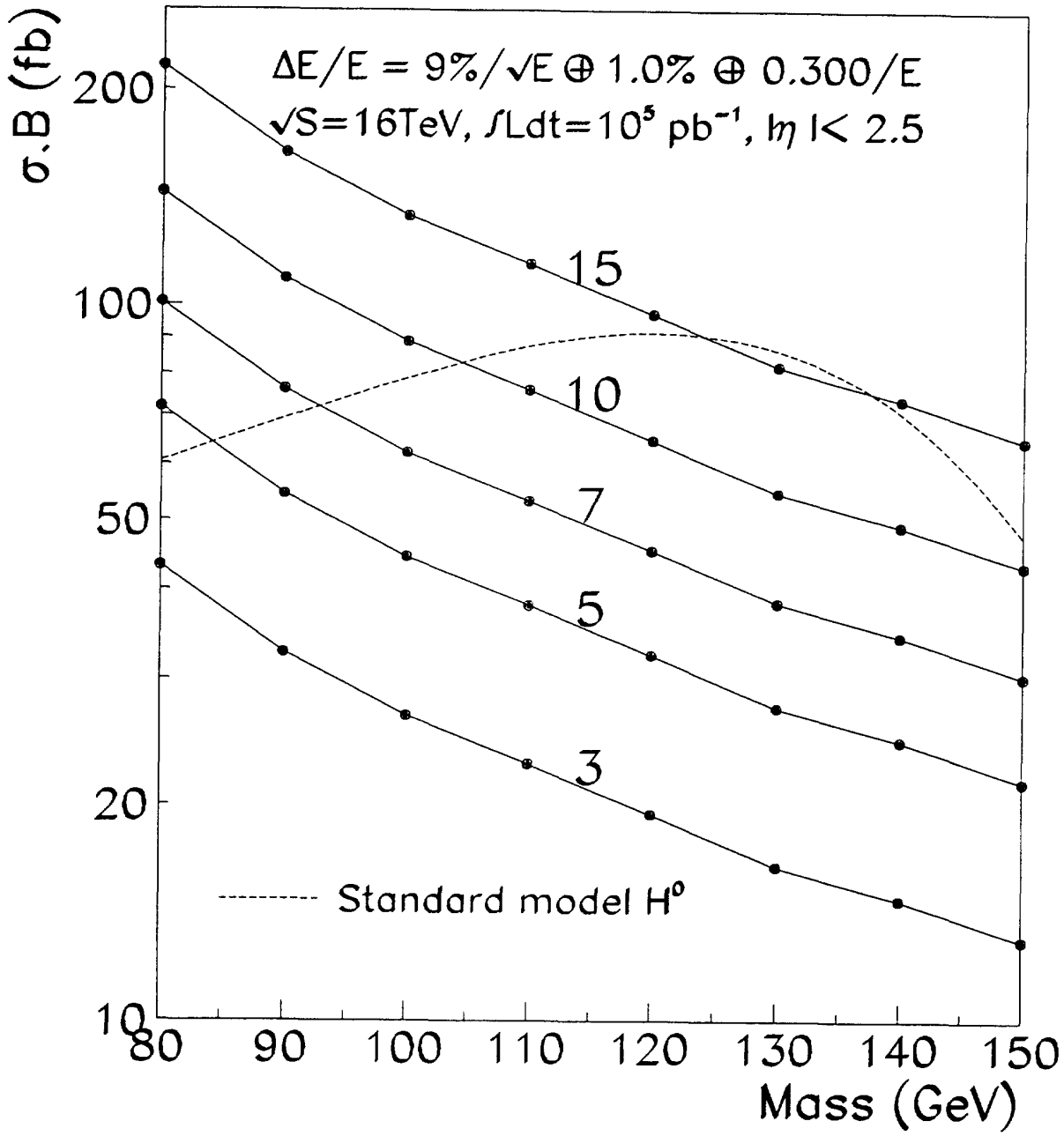

Figure 14: Signal significance in the $H \rightarrow \gamma\gamma$ channel after 10^5 pb^{-1} delivered to CMS Shashlik ECAL.

A signal with a statistical significance of more than 5 sigma would be expected from a Standard Model Higgs for $m_H > 85$ GeV. Figure 15 shows the result of a single Monte-Carlo experiment for 10^5 pb^{-1} and illustrates how SM Higgs of masses 90, 110, 130 and 150 GeV would look after background subtraction. For more details of this analysis see reference[28] and references therein.

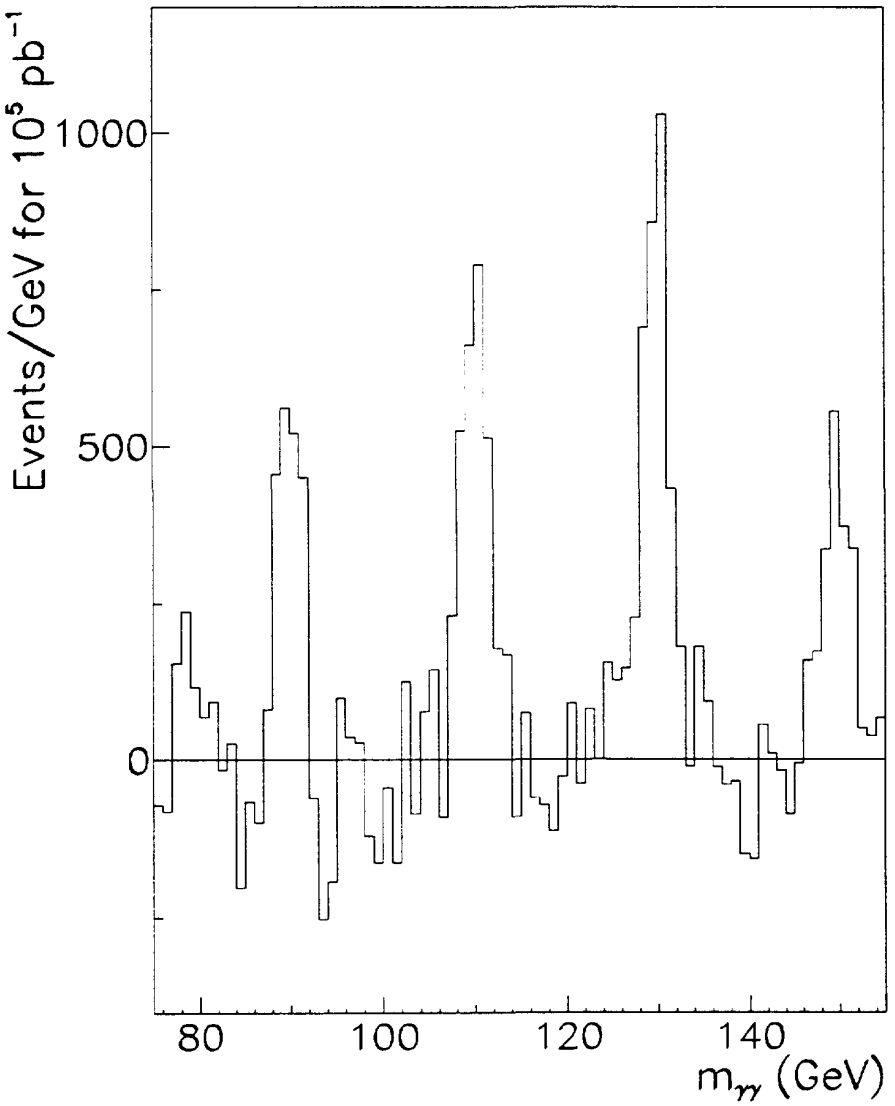

Figure 15: Result of a single Monte-Carlo experiment for 10^5 pb^{-1} with Higgs peaks at 90, 110, 130 and 150 GeV.

[28] CMS Letter of Intent, CERN/LHCC 92-3, LHCC/I1, October 1992

6. Main objectives of the present R&D.

Further R&D should involve the investigation of the following:

- lateral uniformity of response in projective towers,
- radiation tolerant combinations of scintillator and WLS fibres,
- mechanical design of an ensemble of Shashlik+Preshower detectors ,
- quality control of various components,
- methods for monitoring the response of the ensemble over a long period.

6.1. Optimization of the tower parameters.

6.1.1. Shashlik electromagnetic calorimeter for CMS.

The two main parts are:

- the Barrel $(|\eta| = 0 \longrightarrow 1.65)$
- the two end caps $(|\eta| = 1.65 \longrightarrow 2.5)$

The transition between the Barrel and the End caps is not yet well defined. A large number of cables have to be taken out, leading to a crack that can be either projective (and covered by HCAL) or non-projective.

We have concentrated on the Barrel which covers 90% of the solid angle and where the radiation levels allow the use of the Shashlik technique without many problems. The barrel will have projective towers. At high luminosity, a second point has to be measured using a preshower detector to give the shower direction. The preshower should be considered as a separate detector whose effect on overall energy resolution has to be well understood.

CMS constraints stem essentially from overall compactness and the presence of a high magnetic field of 4 Tesla. The first one limits allowed space for the electromagnetic calorimeter in the Barrel region to ~ 600 mm between the inner tracking and the hadron calorimeter. The second one imposes a photo-sensor that can work in a magnetic field. The baseline solution uses Si photodiodes which lead to an appreciable electronics noise. Therefore, the light yield provided by the scintillator must be maximized.

Spatial constraints lead to a depth of ≤ 40 cm for the calorimeter itself. Good light yield requires the ratio K (scintillator volume versus the lead volume) to be as high as possible. The desired energy resolution fixes the sampling frequency. Hence the thickness of the lead plates and the scintillator plates are determined. A compromise satisfying the contradictory needs of compactness, high light yield, good energy resolution and acceptable number of elements leads to the choice of parameters listed in table 4.

Minimum tower depth at $\eta = 0$.	25 X_0
K	2
Thickness of the lead plates	2 mm
Thickness of the scintillator tiles	4 mm

Table 4: Main parameters. of the barrel electromagnetic calorimeter.

The mean radiation length is 16.9 mm and the Moliere radius is 34 mm.

Prototypes produced according to these parameters were tested in an electron beam. The results reported in section 3 are satisfactory through some optimization can still be carried out.

6.1.2. Tower granularity.

The parameters involved here are: the occupancy, the Moliere radius of the medium and the cost related to the number of channels. We propose a front cross section of towers to be~40 x 40 mm^2 corresponding to:

$$\Delta\eta = \Delta\Phi = 0.03$$

Both simulations and tests indicate that the lateral position of the shower barycentre can be measured to better than 1.5 mm at the tower center for 40 GeV electrons. There are 216 towers in Φ and 110 in η ($/\eta/\leq 1.65$). The total number of towers for the barrel part of the calorimeter is 23760.

6.1.3. Depth of the calorimeter.

We have limited the depth of the calorimeter at $\eta = 0$ to 25 X_0, although one would prefer to have 30 X_0. However, it is possible to increase the depth of the towers as function of η. We propose to increase smoothly the depth of the towers up to 30 X_0 at $|\eta| = 0.75$. Above this value and up to $|\eta| = 1.65$, all towers will have a constant depth of 30 X_0.

6.1.4. Tower segmentation.

Although the fact that longitudinal segmentation of towers would improve the calorimeter performance (position reconstruction, π/e separation..) we do not foresee any segmentation for both technical and obvious financial reasons (increase in readout channels).

6.1.5. Light collection.

a) Geometry of the fibres.

The towers have a projective (truncated pyramid) shape. We propose to keep the WLS fibres parallel to the axis of the tower. The light collection is not much affected. The collection efficiency decreases as an inverse function of the tower depth but is more or less compensated by the attenuation length of the WLS fibres. The choice of parallel fibres simplifies the scintillator and the lead manufacture.

the attenuation length of the WLS fibres. The choice of parallel fibres simplifies the scintillator and the lead manufacture.

b) Reflective ends.

Ideally, the fibres should be readout at both ends because of the longitudinal shower fluctuations. Indeed, due to the finite fibre attenuation length such fluctuations induce a constant term in the energy resolution function. The situation can be improved, either by aluminizing one end of the fibres or by making U-loops and hence effectively reading both ends. The use of loops is less difficult and more reproducible though both techniques need to be studied.

c) Number and diameter of the fibres.

For a solution using loops, the number of fibres going through a tower must be the square of an even number, i.e. either 16 or 36. In prototypes tested in beam, we had 25 fibres of 1.2 mm in diameter for a tower of 47 x 47 mm^2. We have shown (section 3) that the light yield was adequate. Twenty five fibres of 1 mm in diameter for a tower of 40 x 40 mm^2 is an homotetic and hence the efficiency of light collection does not change. For a tower of a given lateral size, the light yield scales as n*d (where n is the number of fibres and d their diameter). Therefore, we propose to use 36 fibres with a diameter of 0.83 mm, rather than 16 fibres with a diameter of 1.8 mm, for reasons of channeling and uniformity.

d) Number of diodes per tower.

Two configuration can be envisaged:

- one diode optically coupled to the 36 fibres,
- several diodes each one optically coupled to several fibres.

Electronic noise considerations favor the first solution. However, from a technical point of view, the second solution offers some advantages. Bundling 36 fibres together could be difficult to achieve and needs machining of the bunch after assembly of the tower.

For the moment, we are working on both configurations and will test them thoroughly.

6.1.6. Tilt of the towers in Φ.

This is an important point. From test beam results, it was shown that to avoid channeling, it was necessary to tilt the towers by a small angle (2-3 degrees has been measured to be sufficient). However, our test conditions were not fully representative (no magnetic field, no preshower in front of the tower, larger diameter of fibres than the one foreseen in the final towers).

6.1.7. Tower production.

Figure 16 gives a full design of a Shashlik tower and figure 17 illustrates tower details.

a) Mechanical components.

Each tower is made out of:

- 1 front and rear part in aluminum produced by injection molding.
- 70 to 84 lead plates according to its position at given η.
- 70 to 84 scintillator plates.
- 140 to 168 white paper sheets .1 mm thick.

Two thin aluminum foils (25-30μm thick) will be glued to the lead plates for mechanical construction.

b) Tower assembly.

Using appropriate tooling, the components in a tower are aligned and put under compression (~0.6 bar). Elasticity of the components allows the total length to be brought to its nominal value to within $\pm$0.2 mm.

The respective dimensions of lead and scintillator plates are such that scintillator plate edges are set back a bit from lead plate edges. After putting the glue on the lead, the whole assembly is wrapped with the aluminum sheets. The compression is released once the glue has hardened. The towers are stiff and can be manipulated. The tower lateral dimensions have to be within $\pm$15 μm. Figure 18 explains the assembly principle of a tower. In this assembly option **each lead plate must be at its nominal design position to within 100 μm.** This is only possible by selecting the different parts, measuring their thickness and finally by correct shimming with extra sheets of paper.

c) Holes for WLS fibres and monitoring fibres.

The light produced by a shower in the scintillator plates is readout by 36 WLS fibres of 0.83 mm in diameter, all parallel to the tower axis. The pitch between fibres is around 7 mm. They are introduced into the towers after the tower assembly described above. This requires that all the holes are well aligned. The drilling must be done precisely, to within $\pm$5 μm.

For monitoring, we intend to insert between 2-4 clear quartz fibres in each tower.

d) Machining of the components.

Only the edges of lead and scintillator are machined. Due to the required alignment of holes, the drilling must be done first. The correct lateral dimensions of the lead and scintillator plates are obtained by machining. The holes are used as a reference for this procedure. Steel rods are used for final mounting and wrapping and remain in place until WLS fibres are inserted.

e) Cracks between two adjacent towers.

The mean thickness of glue between towers is foreseen to be around 50μm. Cracks from lead to lead would be then around 200μm (total of 100 μm for the glue and 100 μm for aluminum).The scintillator to scintillator separation between adjacent towers will be ~300μm.

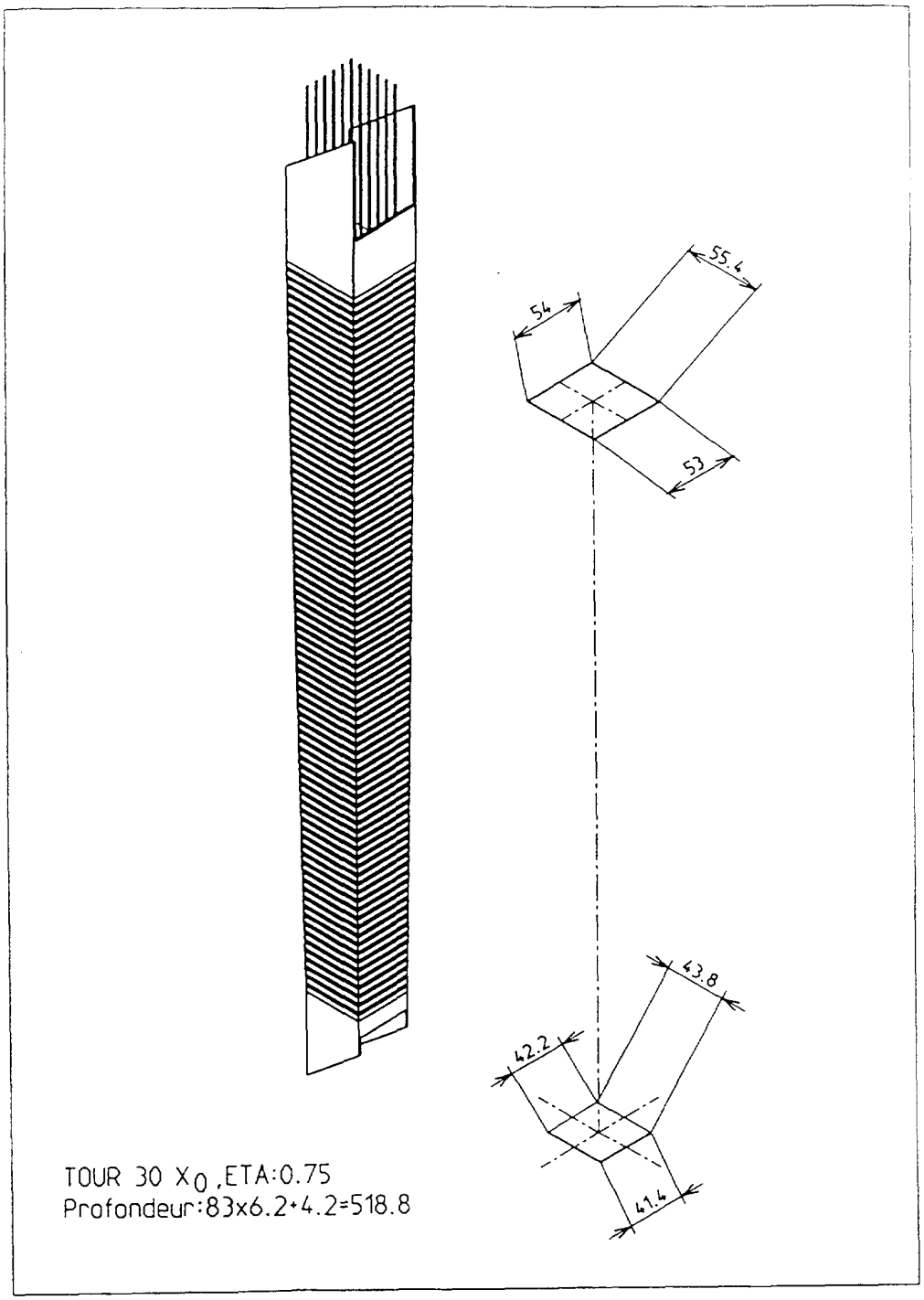

Figure 16: Shashlik tower design.

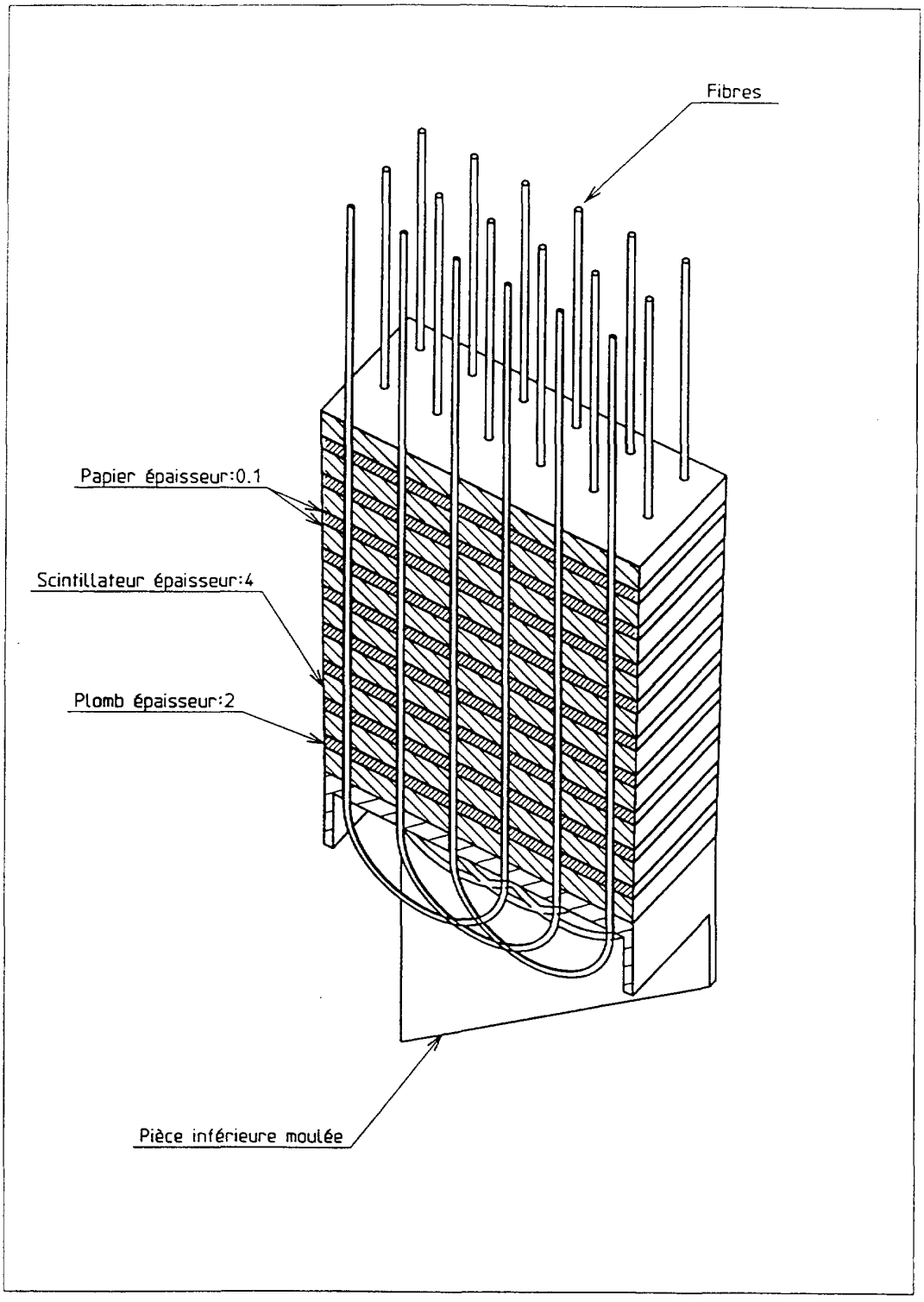

Figure 17: Details of a Shashlik tower assembly.

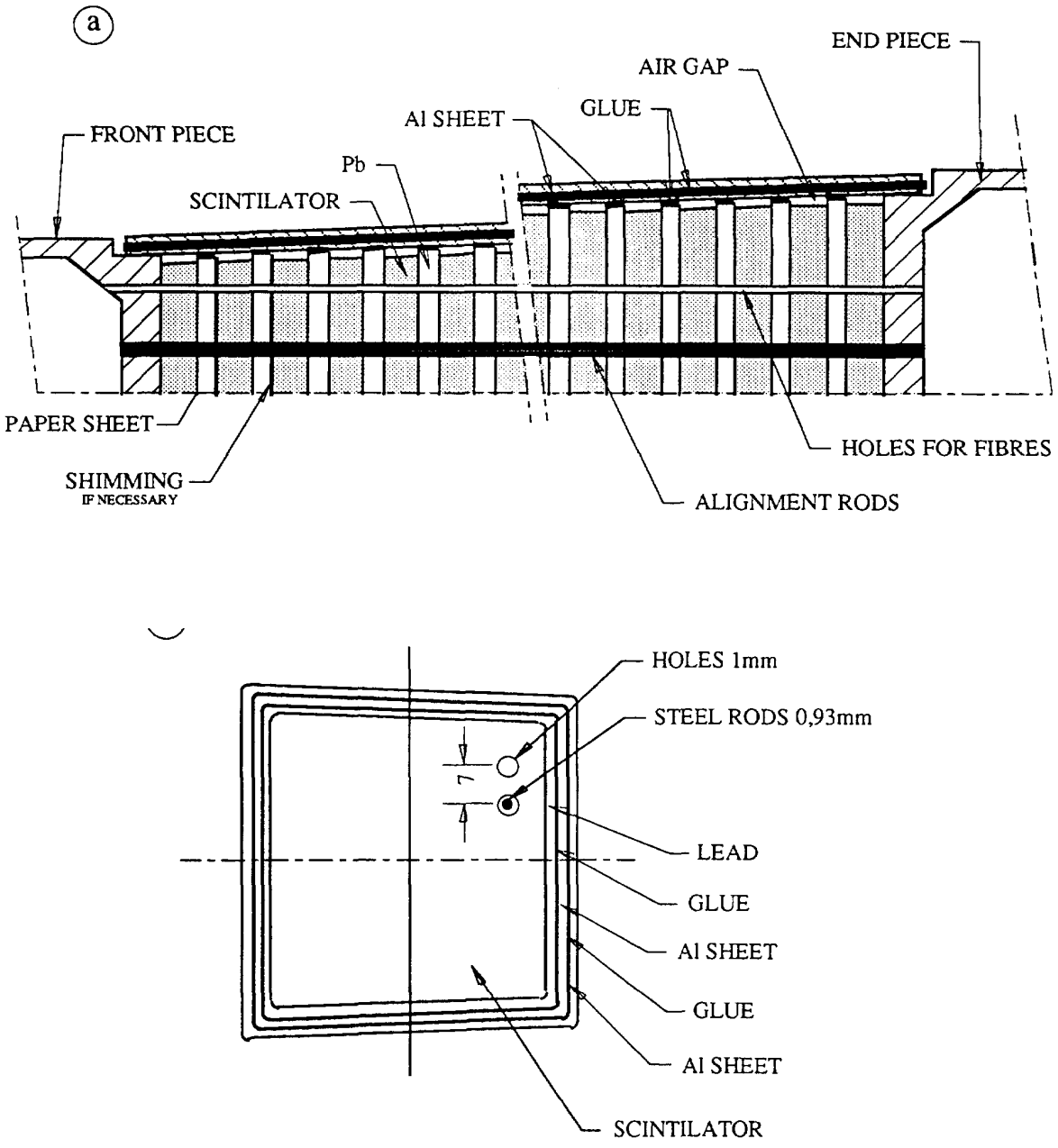

Figure 18: Principle of a tower assembly.

6.1.8. Barrel Mechanical design: Option 1.

We consider here two main guide lines:

• the absorber material, i.e., the lead, must as far as possible, participate in the mechanical stability of the detector.

• the cracks between towers must be minimized for hermeticity and uniformity.

Considering the first point, one can achieve mechanical continuity of the lead plates of the different towers in both η and Φ directions. As a consequence, the optical and mechanical boundaries of a tower have to be glued to each lead plate on the four sides. For optical reasons, and in order to satisfy the second point, the mechanical boundary of towers is made of a thin polished aluminum sheets of 50 to 70μm thick. All the towers are then glued together. This achieves the mechanical continuity of the lead. Special care has to be taken when producing towers. Their dimensions must be kept within tight tolerances, in order to ensure that lead plates of adjacent towers are against each other.

The calorimeter itself is surrounded by an internal and an external cylindrical shell creating a self supporting barrel.

Figures 19 and 20 show the proposed geometry in η and Φ for the barrel. Figure 21 sketches the principle of the gluing assembly procedure.

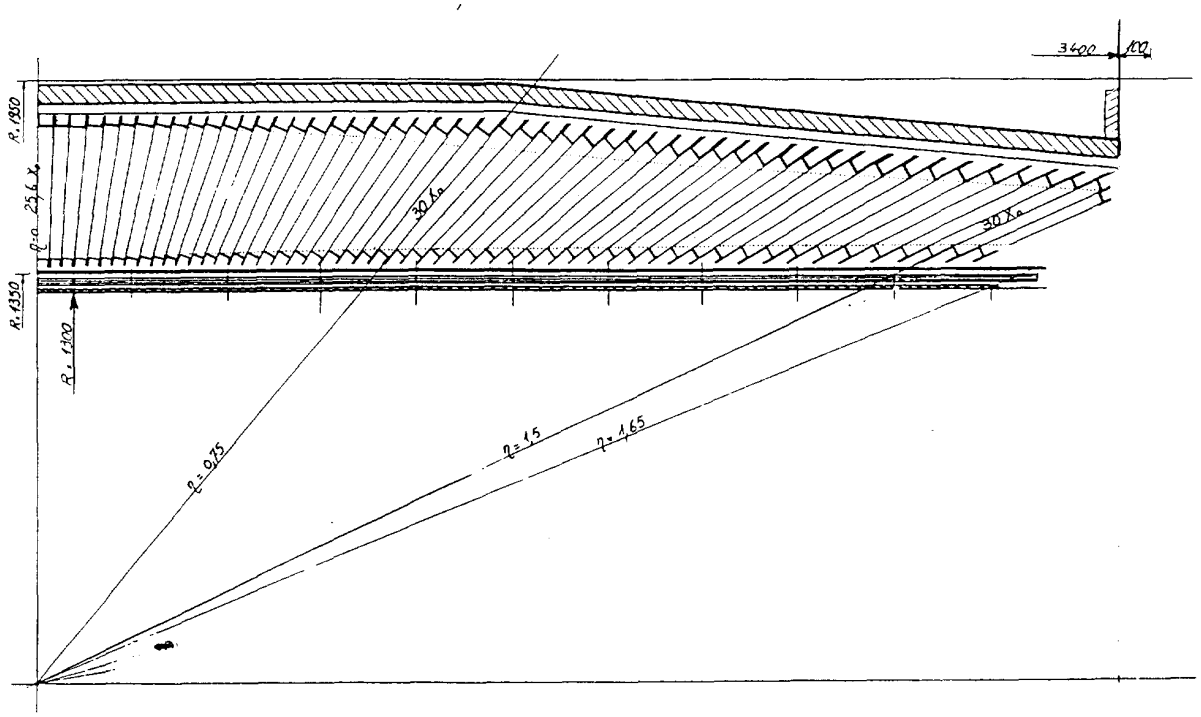

Figure 19: Barrel η view.

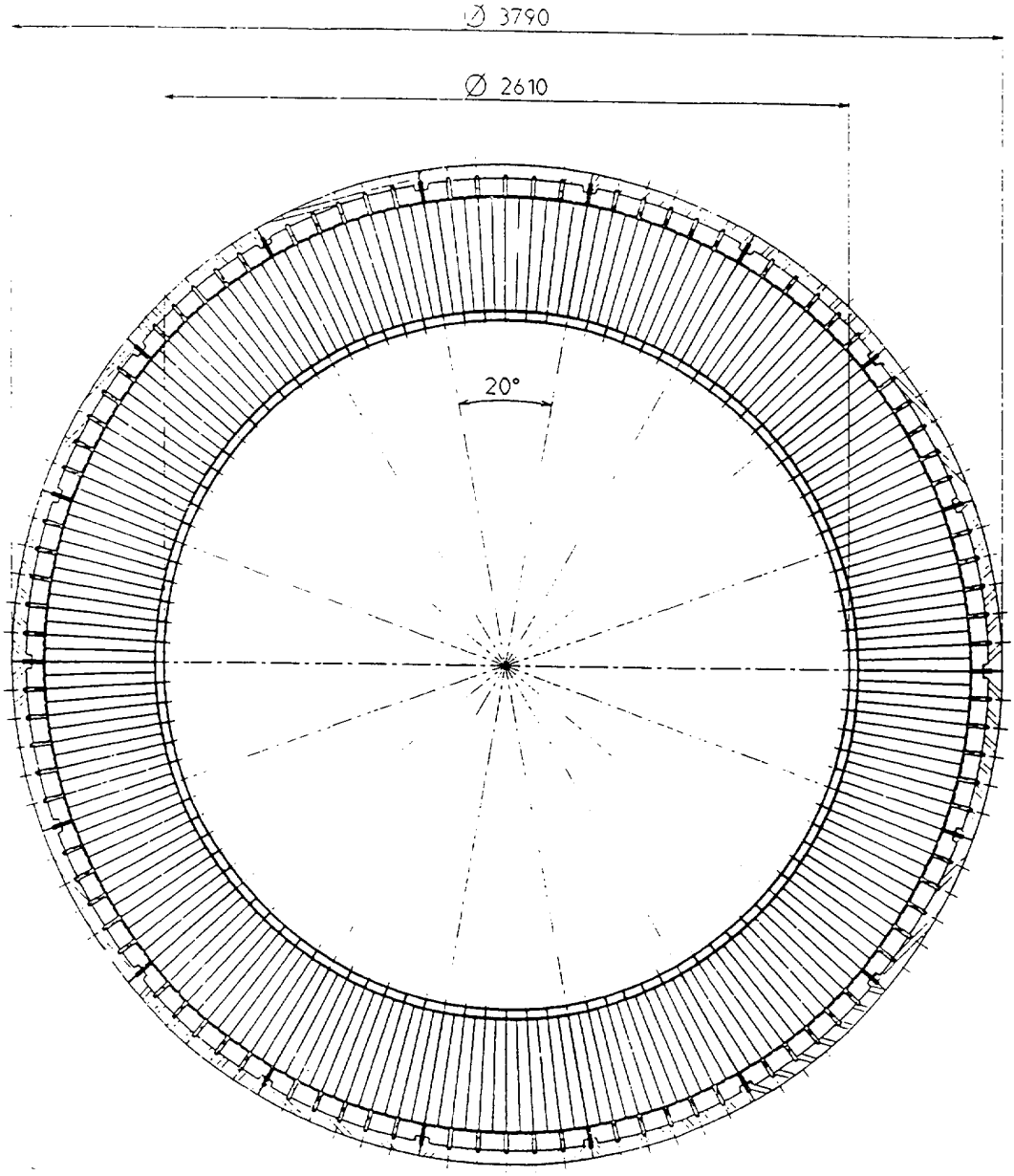

Figure 20: Barrel Φ view.

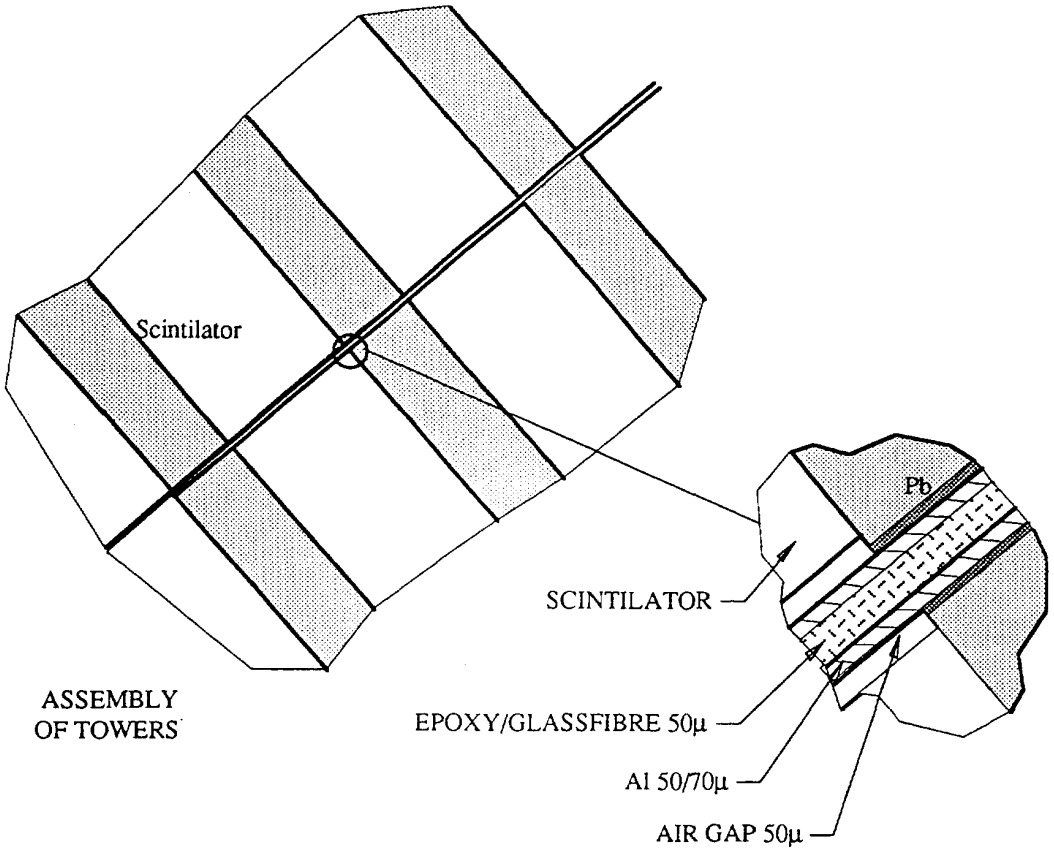

Figure 21: Principle of the gluing procedure.

6.1.9. Barrel subdivision.

Due to its dimension and weight, the detector has to be divided into independent parts. We propose the following:

- Subdivide the barrel into two parts,
- Each half barrel is made out of 18 sectors (20^{o} in Φ) assembled by gluing, after full beam test and calibration of each sector. Production of 40 sectors has to be foreseen including spares.
- The weight of each sector is roughly 3 tons. It is made out of 12 towers in Φ and 55 towers in η, all glued together while mechanical adjustment ensures the correct geometry. At this stage, all the towers are equipped with their readout and should have been thoroughly tested before gluing.

One sector should be representative of the whole detector.

Figure 22 shows the barrel subdivision into sectors.

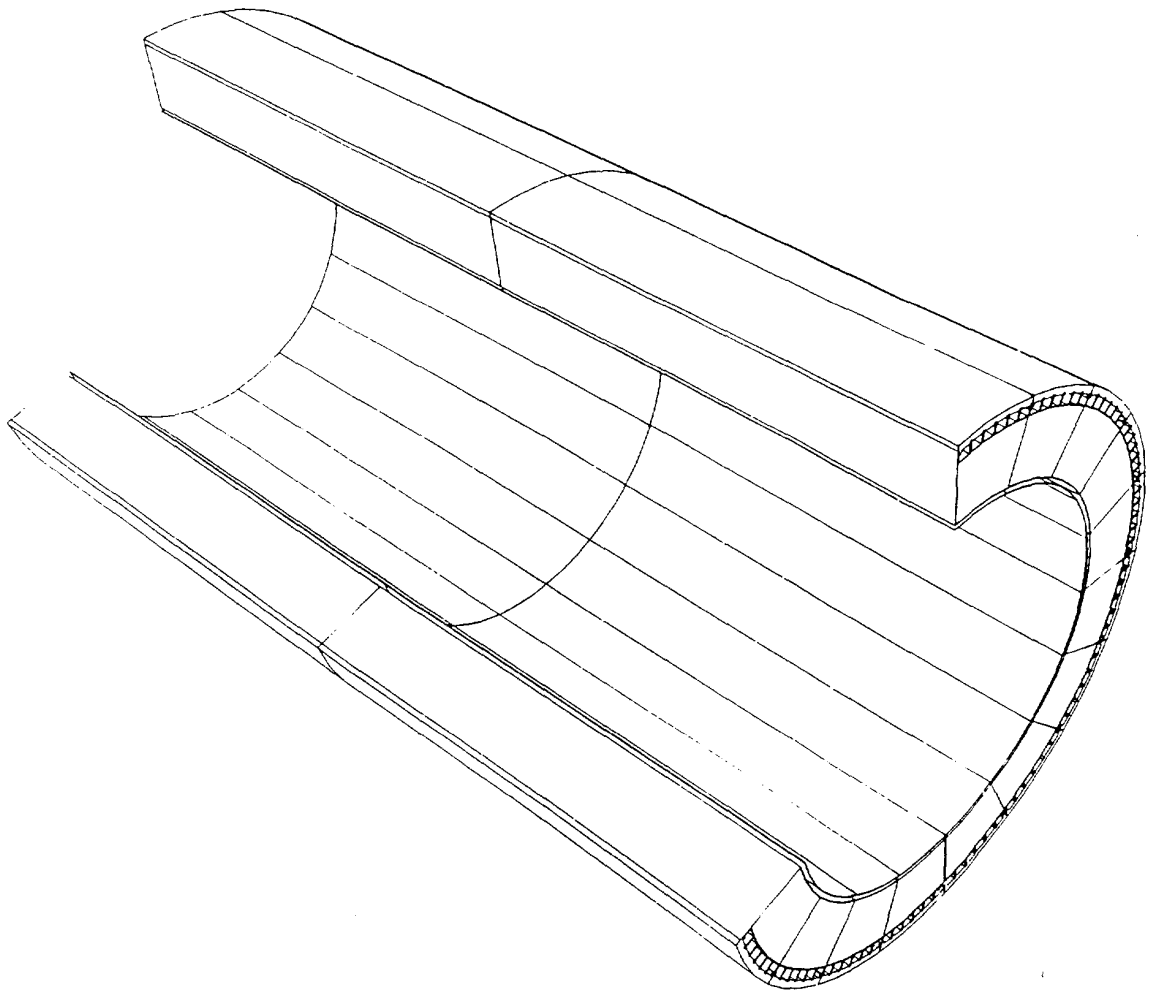

Figure 22: The barrel sectors.

6.1.10. Barrel Mechanical design: Option 2.

An alternative solution is an extension of the work carried out at RAL on support systems for a crystal tower calorimeter.

a) Support system for tower construction.

Two alternative design approaches have been initiated to identify the most suitable and cost effective method of constructing the cylindrical barrel section of the ECAL using Shashlik towers as individual detector elements. The first design approach described earlier is based on a sequential gluing operation where several adjacent tower elements are glued together initially to form larger sub modules suitable for calibration and assembly into the final detector in the intersection region surface hall. The number of towers chosen to form a sub module in this approach is dictated by the need to define an acceptable modularity for handling purposes and for subsequent assembly into an overall glued up cylindrical barrel detector. This approach, as described in the previous sections, is attractive given the minimum amount of mass introduced by support system but it does however require very high tolerances both in manufacture and in assembly techniques and could prove to be extremely difficult and expensive to implement in practice.

To ensure that an alternative construction and support system is available, should it prove impractical to adopt the glued approach, a second design study will be undertaken at RAL to investigate a suitable support system for the cylindrical barrel section of the ECAL. This approach will be based on the use of either individual pockets or some form of super pocket lattice structure. The previous work carried out by RAL[29] on a similar system for a calorimeter using crystal towers as the individual elements and the carbon fibre lattice support produced for the L3/BGO calorimeter[30] which although smaller in scale than the support system required for the CMS ECAL are both indicative of the possibilities of such an approach.

b) Overall structural support for the barrel section of the electromagnetic calorimeter.

The overall support and installation planning for the barrel section of the ECAL are still basically as outlined in the LOI. In this planning, the cylindrical section of the ECAL is supported by a primary rail system mounted on the inner bore of the HC. The ECAL mounting structure in turn must be designed to provide support for the installation of the preshower and inner tracker detectors which have to be mounted within the inner bore of the ECAL. The design of this secondary support structure is made more complicated by the need to accommodate the staging proposals for the preshower detector. This planning requires that the preshower detector be installed at later date after start up without the need to move the ECAL. The installation of the staged preshower detector being achieved by removal only of the inner tracker from the inner bore of the

[29] Initial Finite Element Analysis of a Support for the CMS Electromagnetic Calorimeter.
RJS Greenhalgh, IG Denton, DJA Cockerill. Rutherford Appleton Laboratory. CMS TN/93-61.
[30] Progress of the L3/BGO Calorimeter. M Schneegans NIM A257 (1987) 528-537.

ECAL. Such a scenario defines the need for a special support system for the combined preshower and inner tracker detector array with facility for withdrawal from inside the ECAL.

The combined weight of the three detectors is estimated to be approximately 130 tons with the total weight being transferred through the detector array to the outer support and ultimately onto the primary rail system. The preliminary design studies shown on figure 23 indicate the type of outer support structure envisaged at present .

c) Conclusion.

In both design studies RAL will provide experienced design staff with previous experience of design and manufacture of large scale detectors for the LEP programme. The design teams at RAL will have access to modern CAD tools including 3D layout and FEA to allow quantitative analysis to be carried out on any proposal.

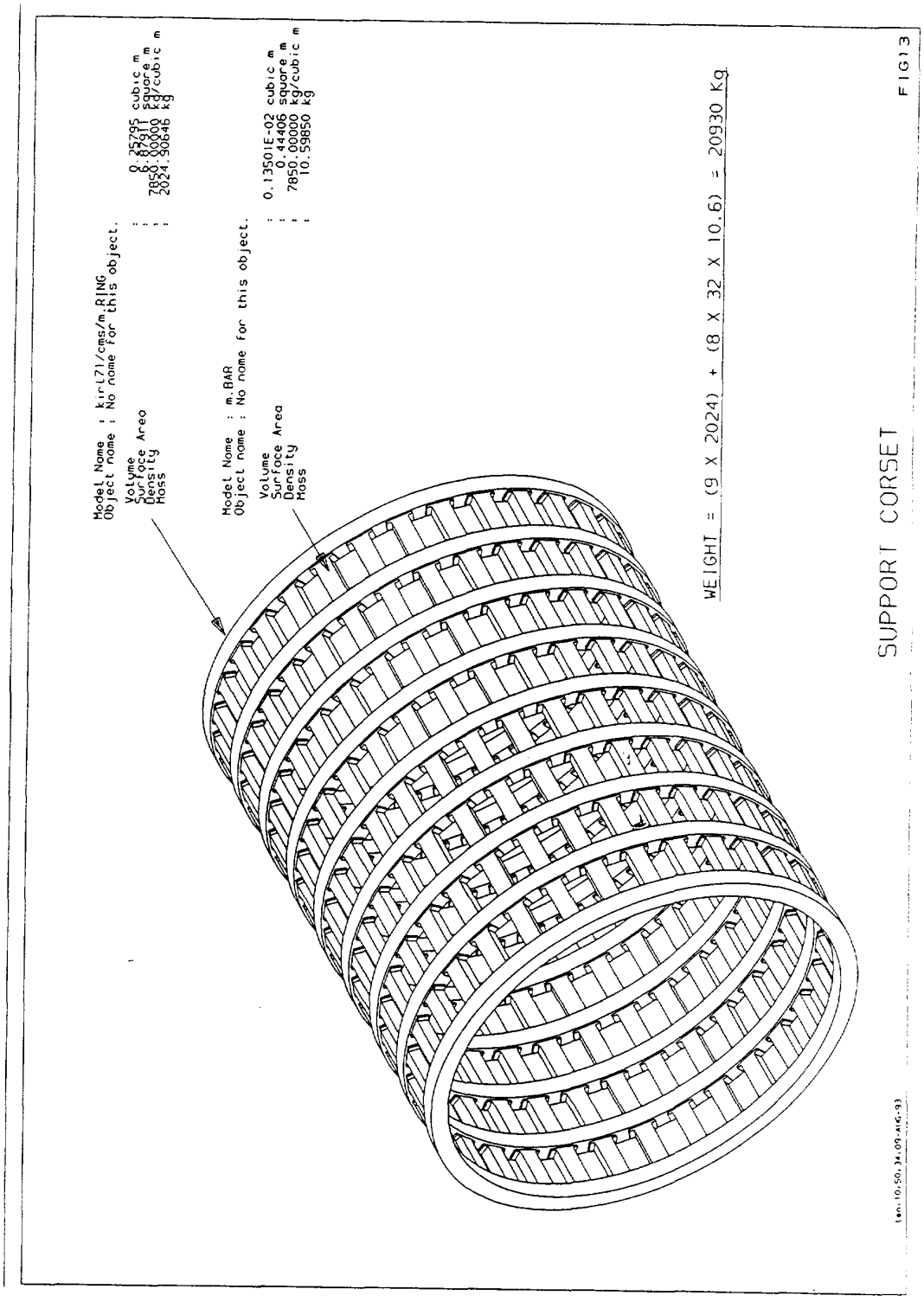

Figure 23: Type of outer support for the Shashlik ECAL.

6.1.11. Mechanical prototypes.

Mechanical prototypes are needed for the study of the mechanical stability of the barrel obtained with the construction methods described above. A finite element calculations of the ECAL need to be carried out. They will be carried out by RAL and the Detector Support group from DAPNIA (Saclay). The latter are involved in the design study only.

In order to carry out this program, we intend to fabricate a certain number of identical towers 30 X_0 in depth of pyramidal shape. Their dimensions will reflect towers sitting at $|\eta| = 0.75$. Their cross section is chosen to be square in order to minimize the tooling needed for the assembly and gluing. All components of the towers must be identical to the real one except front and rear aluminum parts, the shape of which will be a simple plate of equivalent thickness.

6.1.12. R&D objectives.

The main goals of the present R&D arise from the question as to how best realize the holding structure using the Shashlik towers. They are:

- Demonstrate that the glued solution at the level of a tower is realistic and would work in the LHC environment.
- Construct a finite number of mechanical prototypes to define the tower construction techniques.
- Answers to the above questions will allow us to choose the optimal mechanical structure for the calorimeter.
- Other types of prototypes for evaluating the calorimeter performances have also to be constructed and tested in an electron beam.

6.1.13. Quality control.

We will rely and benefit from the control procedures laid down in the Delphi "STIC" project.

The parameters to be measured and controlled for the tiles production are :

- Mechanical accuracy, including tile dimensions, the hole position and radii etc. A bubble-chamber measurement table can be used, as demonstrated by the "STIC" project of Delphi[31] . The parameters may be stored in a data base and tiles may be subdivided into groups to provide the desired mechanical accuracy of the towers.
- An important factor which could cause systematic variation in the response from tile to tile and could be responsible for aging effects is the mechanical stress which has been built into the plastic when cooling it after the injection into the mould. It is possible to develop a simple device which indicates the level of stresses by measuring the birefringence of the tiles by placing the tile between two Polaroid filters with the polarization axes rotated by 90 degrees. The parameter that

[31] Prototype design, construction and test of a Pb/scintillator sampling calorimeter with WLS readout" contr. to IEEE conf, Florida,1992

could be measured is the total light that gets through the filters. Smaller stresses lead to smaller amount of light transmission. Such a test was proposed by Delphi NEC group[32].

• The light output from the tiles may be controlled by using a bundle of fibres, which are inserted into the holes and the bundle is connected to a PM. The tile is irradiated with a collimated source and the PM current is measured. The Delphi STIC group have demonstrated the effectiveness of this method. Not only can the average light output be measured in this way but also the variation.

• WLS fibres quality control may be organized either by measuring the attenuation curve by scanning the fibre with a light source(the light may be produced by a small scintillator irradiated by the source), or by measuring an optical properties of the fibre like, for example, numerical aperture, which is very sensitive to all possible quality fluctuations like non parallelism of the fibre walls, local problems at the core-cladding junction, non uniformity of the refractive index etc.

• checking the tiles and the fibres is not sufficient to guarantee a uniformity of response compatible with the goal of building a calorimeter with a 1% constant term. After assembly of the tower a collimated radioactive source can be moved longitudinally along one of the edges. A PM can be used to monitor the current. This measurement should allow quantification of the longitudinal uniformity of response.

The development of the quality control stations is an important part of the proposed project.

[32] (Delphi 92-31 Phys 166)

6.2. Readout electronics[33] for the calorimeter.

6.2.1. Introduction.

The 36 WLS fibres can be grouped onto a single or several photodiodes. The latter solution leads to a saving of space. However electronics noise equivalent may increase.

6.2.2. Silicon photodiodes readout.

a) Photodiodes matrix.

INTERTECHNIQUE (France) have provided us with different detector types: 2x2, 3x3 matrices and individual photodiodes.

The main parameters and characteristics of these detectors are given in table 5.

Origin of Silicon	Wacker
Resistivity	from 5000 to 8000 Ω.cm
Structure: PIN	Thickness = 300μm
P zone: Bore implant	Thickness = 500 A
Anti reflection layer	None
Diameter of the effective area	1.2 mm
Width of the aluminum upper electrode ring	0.2 mm
Matrix pitch	5 mm

Table 5: Main parameters and characteristics of the detectors furnished by INTERTECHNIQUE.

b) Interconnections.

A matrix detector can either be made on a silicon wafer or from interconnecting single SiPD's mounted on a printed board. The "full silicon" matrix is interesting if the dimensions of the matrix are small. In our case, we have to use the second solution. The diodes are mounted on a printed circuit board. The measured capacitance for a 3x3 matrix of a "full silicon" wafer varies between 20-30 pF for different types of interconnection. For comparison, the measured capacitance for a single SiPD mounted is 2.5 pF.

c) Measurements results.

Different parameters have been measured with the detectors furnished by INTERTECHNIQUE. They are summarized below:

• *Quantum efficiency.* We obtained 56% at 550 nm. This low value is explained by the fact that we had no anti reflection layer. About 30% of the incident light was reflected.

• *Leakage current.* We measured 3 nA/cm^2 at 20 °C for a bias voltage of 60 volts.

[33] Readout electronics for the Shashlik calorimeter. CMS TN / 93-76.

• *Series resistance.* For the 3 x 3 matrix we measured a resistance of 10 to 20 Ω. This is relatively high. A series resistance smaller than 10 Ω is needed for the detector.

• *Capacitance.* The measured capacitance is 1 pF for 1,6 mm diameter diodes.

d) Noise measurements.

The noise due to the SiPD matrix was measured with a discrete components JFET amplifier which will be described in the next section. We made the measurement with a 3 x 3 matrix of a "full silicon" wafer. The interconnection between diodes were of thick oxide type. The measured capacitance of the setup was 29 pF. The results gave a 17% additional noise to the one measured for the preamplifier with the same input capacitance. This is mainly due to the relatively high series resistance of our detector. Our JFET amplifier with its high g_m (> 10 mmho) is very sensitive to the series resistance as it will be shown here after. The quantum efficiency of the INTERTECHNIQUE detectors has to be improved and the series resistance decreased. We plan to compare the performance using matrix and single diode solutions.

6.2.3. Low noise preamplifiers.

a) Discrete component amplifier.

For the test beam results presented in section 3, we used a JFET amplifier designed at INR (Moscow) shown in figure 24. The equivalent noise charge (RMS) for this amplifier versus detector capacitance is given in figure 25. One sees that for C_D = 30 pF and a τ_{RC-RC} = 10 ns, an ENC of 1100 e- is measured.

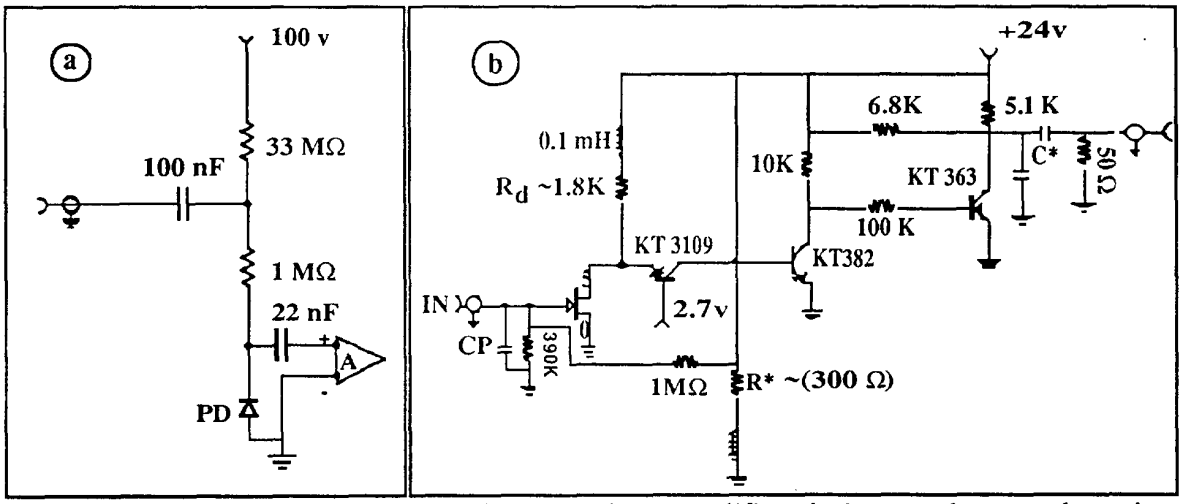

Figure 24: Photodiode power supply (a) and preamplifier design used to readout the CMS prototype Shashlik towers (b).

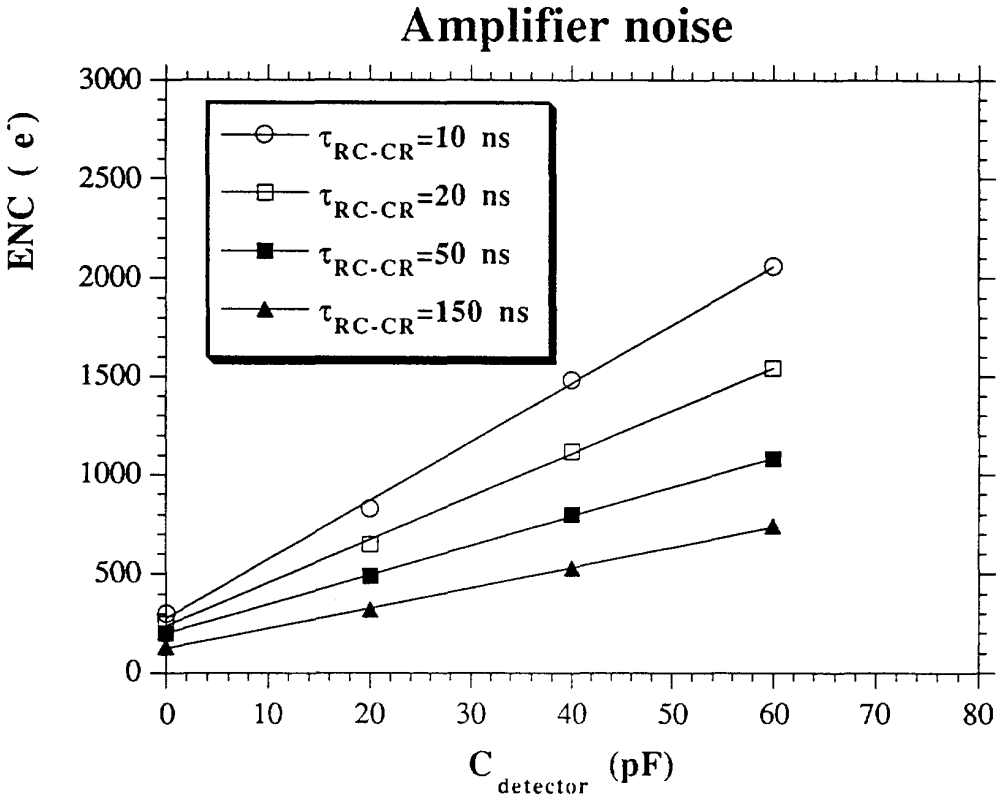

Figure 25: Equivalent noise charge (RMS) for the amplifier shown on figure 24 versus the capacitance of the detector.

b) R&D objectives.

• Our collaborators from INR have developed a hybrid version of the discrete amplifier shown in figure 24. It will be tested in our next test beam periods (August and October 1993).

• Other versions of amplifiers are under development at Rutherford and at INP Lyon.

6.3. R&D on preshower detector.

Preliminary results from the test beam data indicate promising angular resolution for the Shashlik+Preshower combination, while the energy resolution of the whole system is not degraded much. These results have to be confirmed by placing the device in the magnetic field.

Precise simulation has to be developed and compared to the data. π^0 rejection has also to be carefully studied, in the beam with and without magnetic field and compared with Monte Carlo.

6.3.1. Main parameters.

The detector is cylindrical in shape for the barrel. It could be either continuous or segmented in plates. It is 7m long, 8-10 cm thick and will have 3 radiation lengths in total. Shower position is measured by Si strip detectors, 2 mm pitch, placed after $2X_0$, and $3X_0$ for the Φ and η position respectively. Overlapping in both Φ and η directions should avoid cracks. The total number of channels is around 500K. The power dissipation is estimated to be between 5-10 kW. Therefore a detailed study of the cooling system is needed. The detector is supported by the ECAL and supports the tracking detector. The total weight is 12 tons.

6.3.2. Choice of the preshower mechanical structure.

Many different options for the mechanical lay-out have been considered. One of them is presented below as an example.

• Two independent cylinders made of lead, are built respectively with $2X_0$ and $1X_0$ of absorber material. The physical thickness of the cylinders decreases as η increases, to keep constant the radiation length seen by the showers (figure 26). The silicon detectors are fixed on each cylinder. The 2 cylinders are joined together with small mechanical pieces. To ensure the rigidity, the first one is sandwiched between 2 aluminum plates of a thickness of 1.5 mm.

In both cases the cooling system (most probably the same as for the inner tracker) can be either included in the radiator or be independent .

6.3.3. Milestones for the R&D.

• Measure the angular and energy resolution of the Preshower + Shashlik system.

• Study the mechanical realization, with special care given to the cooling system.

• Define and study the appropriate rad-hard electronics for the read-out.

For all these studies different prototypes must be built and tested on a beam together with the Shashlik towers.

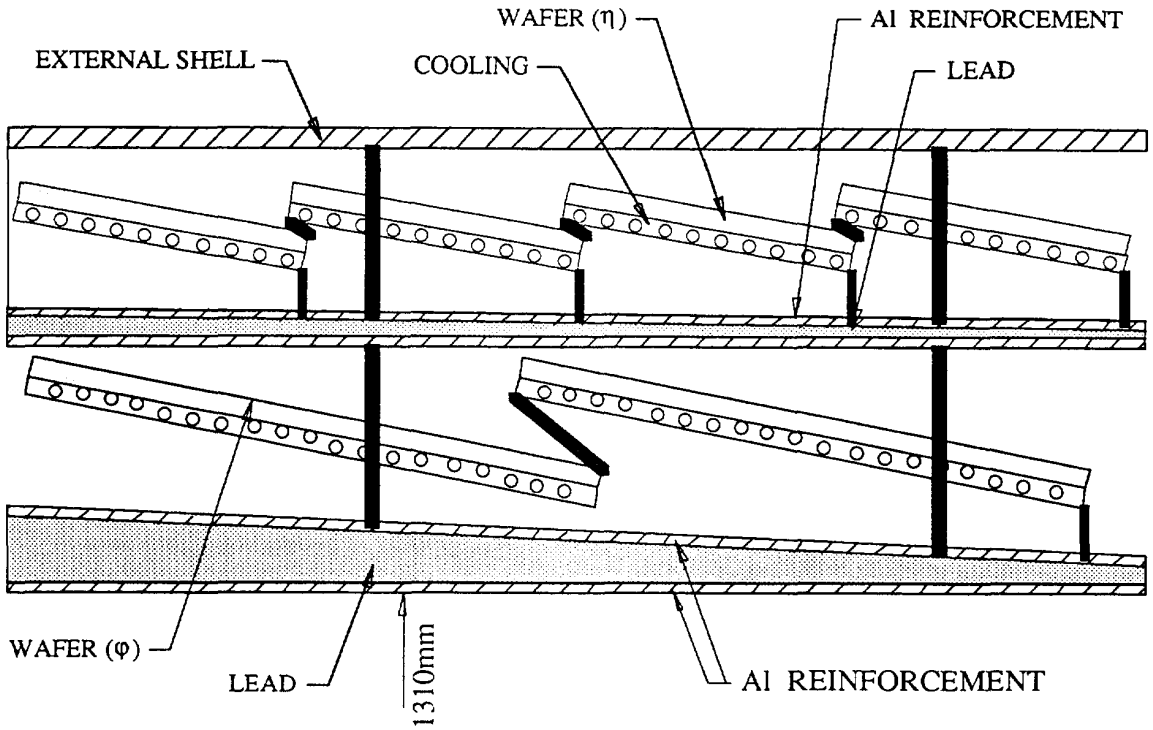

Figure 26: Possible designs of the preshower detector mechanical structure.

6.4. Readout electronics for the preshower.

6.4.1. Introduction.

The preshower detector must have a compact construction and with 500 k channels remote electronics is excluded. Therefore, the front end electronics, in the form of monolithic chips, must be placed directly on the silicon strip detector modules. For this reason, readout electronics based on FLASH digitizers (one per channel) is not acceptable in terms of power consumption and dimensions.

The preshower readout electronics must provide signal processing and sparse data readout at low power consumption (<10 mW) in order limit the data flow to the DAQ system. Such a custom I C electronics system, based on the HARP architecture[34],[35] has been already developed in the framework of RD2 . This readout system utilizes an analog memory technique implemented in VLSI CMOS technology on silicon to store analog signals during the processing time of the level-1 trigger. First developed by RD2 for silicon preshower application[36],[37] [38] this readout electronics has speed, noise and dynamic range performance close to our requirement.

6.4.2. Analog memory readout chip.

A 32-channel analog memory chip , 128 memory cell (3μs of local storage time at 25 ns BCO) with fast current amplifiers ICON[39] compatible with a direct coupling to the silicon strip detector is now available[40]. The chip architecture , shown in Fig. 27 , includes in addition to the analog electronics, all the digital circuits necessary to control the analog memory addressing. The output of the chip provides an analog multiplexed signal of the amplified and sampled input charges of the 32 channels synchronized with the level-1 decision. Write and read operations are performed simultaneously to enable readout with no dead time.

The silicon detector charge is sampled by the analog memory at 40 (66) MHz via the ICON preamplifier with a gain of 10 mV/MIP-300μm-Si. If the detector charge is spread over few BCO, the sum of adjacent memory cells belonging to the triggered event is sufficient to retrieve the full detector signal.

---

[34] P. Jarron et.,al Analog Sampling techniques in CMOS technology, in proceedings of the first Electronics for Particles Physics Lecroy Conference in 91.
[35] E. Heijne et al., Monolithics CMOS front end Electronics with analog pipelines. IEEE Nuclear Science Symposium, Arlington, October 1990.
[36] RD2 proposal CERN/ DRDC/90-27, DRDC/P3. 2 August 1990.
[37] RD2 status report CERN/DRDC/92-4 9 January 1992
[38] RD2 status report CERN/DRDC/93-18 9 March 1993
[39] ICON, M. Campbell, F. Anghinolfi, E. Heijne and P. Jarron., A Current Mode Preamplifier in CMOS technology for use with High rate particle detector. IEEE Trans on Nuclear Science, VOL 40, No3, June 1993, 271-274.
[40] F. Anghinolfi et al., A 66 MHz, 32 channel analog memory circuit with data selection for fast silicon detectors. NIM A326(1993) 100-111.

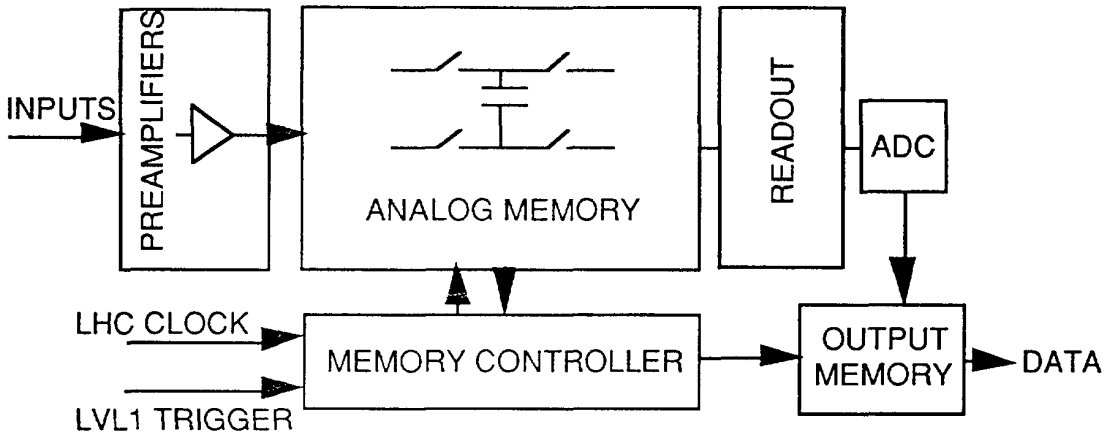

Figure 27: Block diagram of the RD2 chip. ADC is not yet implemented on chip

6.4.3. Specifications of the preshower readout electronics.

Table 6 gives the target specifications required for the preshower electronics; in comparison RD2 chip are given.

Specs	Target specs	Specs RD2 chip
Nb of ch/Chip	32	32
memory depth	128 cell 2-3μs delay	64-128
Si det capacitance	50-100 pF	10 pF
Sampling freq.	40-66 MHz	40-66 MHz
Readout freq.	1-5 MHz	1-5 MHz
Noise ENC @0pF	2000 rms e+50 e/pF	2000 rms e+90 e/pF
Power consump.	10 mW/ch	10 mW
Gain	10 mV/MIP	10-30 mV/MIP
input Rin/Cin	100Ω/15 pF	300 Ω/3pF
Linear range	±2 V	± 1.5 V
Channel occupancy.	1 %	1 %
Nb of cell/event	3-4	3-4
event buffering	8	8

Table 6: Target specifications required for the preshower electronics in comparison RD2 chip.

Target specs are very similar to RD2 chip except for detector capacitance which is one order of magnitude larger due to the larger area of the silicon strip detectors (2 mm width, 60-120 mm length). Preliminary speed measurement of the RD2 chip for 10, 50 and 100 pF detector capacitance is illustrated in fig 28 a , b and c.

RD2 has developed a complete test beam acquisition system based on the analog memory chip described in reference[41]. We plan to use components of this readout system with the necessary modifications for our preshower beam tests in 94. ECP-MIC group will provide us front end chip based on the existing version.

6.4.4. R&D objectives.

The first step is the existing chip by redesigning the ICON amplifier for larger capacitance taking into account a possible trade off between speed and power consumption. Pedestal uniformity and common mode pedestal fluctuations must be carefully studied to ensure a dynamic of 10-11 bits and a linearity of few %.

The present chip can handle detector leakage current of 10 μA which must be improved to 50μA.

Further improvements of the chip architecture foreseen are:

- ICON redesign
- improvement of the precision of the analog memory
- implementation of a 11 bit dynamic range, 8 bit precision A to D converter.
- local digital signal processing to accomplish pedestal subtraction signal summing of triggered memory cells, gain correction
- data formatting and bus interfacing.
- Electronic calibration circuit.
- Leakage current monitoring.

A sparse chip readout is very useful to reduce the front end raw data. We expect to study this possibility by implementing on chip a fast sum of the selected memory cells which the value is compared to a presetable minimum energy threshold. Readout is only performed when sum is above this threshold. ECP-MIC group has the responsibility of this chip development.

6.4.5. Radiation hardness.

Radiation level in the barrel preshower is ~0.5 Mrad and 2 10^{13} n/cm^2 for 10^6 pb^{-1}. These go up to 5 Mrad and 3 10^{14} n at $\eta = 2.5$ for 10^6 pb^{-1}. Special treatment (cooling, replacement...) has to be envisaged for the region $2.0<|\eta|<2.5$. Preliminary results of various groups working on radiation hard electronics (RD9, MPI Munich, CEA-Saclay,RAL...) indicate that radiation hard CMOS monolithic chip amplifier and analog memory (RD9) can easily operate up to levels of radiation in the barrel region. Nevertheless, in our case a relative high precision of the front end is required (11 bits). We plan to carry out a specific study the impact of radiation damage on the precision and dynamic range of monolithic circuit.

[41] R. Bonino et al., Electronics and readout of a large area silicon detector for LHC. to be published in the proceedings of 93' San Miniato conference.

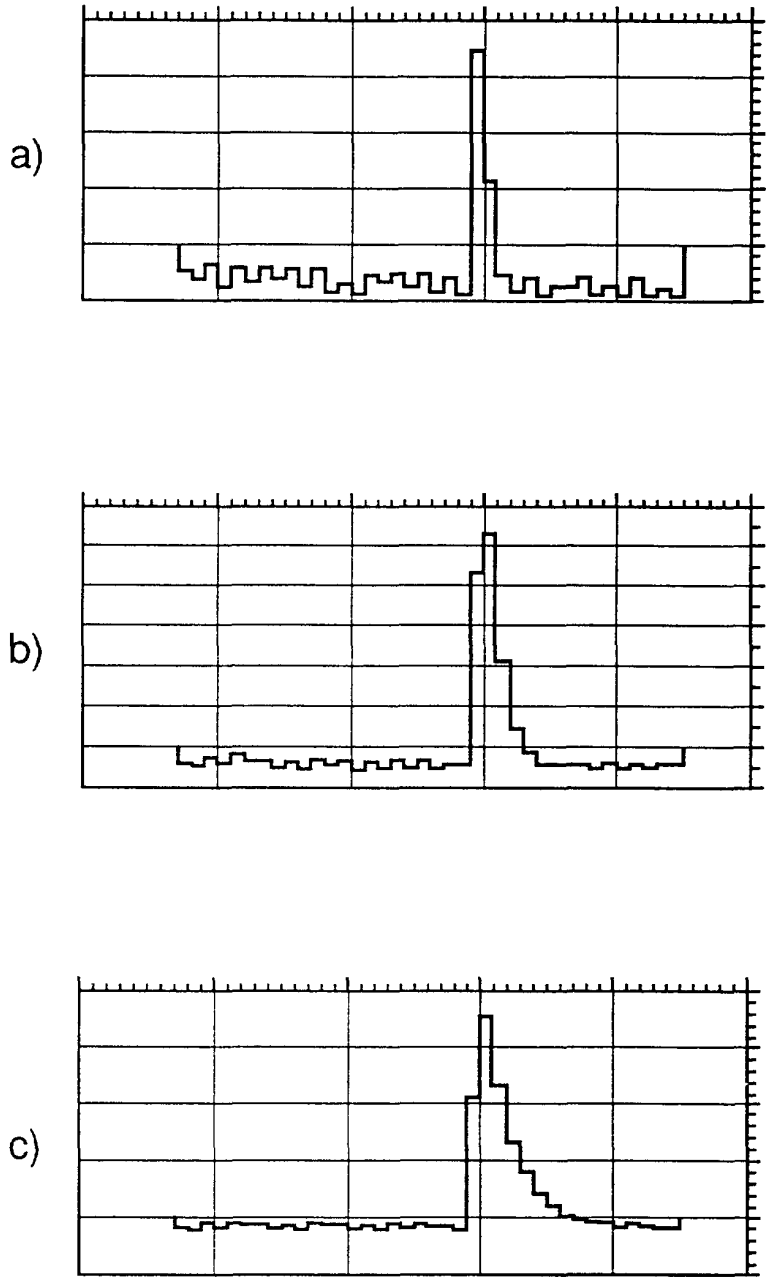

Figure 28: Preliminary speed measurement of the RD2 chip (horizontal scale = 25 ns/bin):
a) $f_{sampling}$= 40 MHz (BCO = 25 ns), C_{det} = 12 pF, Charge spread = 1.5 bin.
b) C_{det} = 50 pF, Charge spread = 3.5 bins.
c) C_{det} = 100 pF, Charge spread= 6.5 bins.

6.5. Calibration and monitoring of the Calorimeter.

A precise calibration system will be required to achieve and maintain good energy resolution in the Shashlik calorimeter. Calibration errors affect the energy resolution and contribute to the so called constant term in the energy resolution formula. Reliable monitoring will be essential for fault detection and for the commissioning and running phases of the experiment.

6.5.1. Calibration.

a) Required calibration precision.

Electromagnetic showers are narrow; between one and (at most) four Shashlik towers will contain >80% of the shower energy. To first order, the lateral shape of electromagnetic showers is constant on a shower to shower basis and as a function of energy. Hence the deterioration of the energy resolution, σ /E, due to inter-calibration errors, will be approximately independent of energy. In order, for the inter-calibration error not to significantly contribute to the constant term the R.M.S. error on the calibration constant for a single tower must be less than 0.4%.

b) Calibration procedure .

We intend to calibrate the complete Shashlik detector at test beams prior to installation at CMS. The subsystems will be fitted with their final readout and monitoring systems. With the test beam measurements, we hope to achieve absolute calibration and inter-calibration of all towers to within 2% at the start of operation at LHC. This corresponds to a constant term of around 1.3%.

This initial calibration is limited by changes which occur to the system between test beam calibration and final installation in the experiment. These changes arise, in part, through disconnection's and reconnections which may alter the signal size for both the calorimeter and the monitoring system. We intend to keep these changes to a minimum by providing dedicated monitoring systems for each of the Shashlik subsystems.

At LHC we will rely on isolated high transverse momentum electrons from heavy quark or intermediate vector boson decays to accomplish, in situ, precision calibration and monitoring. This will be done by requiring a momentum and energy match between the tracker and the calorimeter. The tracker system will be able to measure the transverse momentum of electrons to within 0.5% at 10 GeV and $\leq$ 1% at 50 GeV for the whole of the central region out to a rapidity of 2.0.

The initial calibration will be refined once the experiment begins data taking. At the LHC startup luminosity of 10^{33} cm^{-2} sec^{-1}, each tower will receive about 100 electrons, above a transverse momentum of 35 GeV, in ~5 days from single electron production, for rapidities out to 2.5. A similar number of di-electrons with transverse momenta above 30 GeV, from Z decays, will be received in a similar time at high luminosity.

The calorimeter and tracking information will be taken from events triggered by single (or double) isolated electromagnetic energy deposits and fed into a dedicated on-line analysis chain to

continually update the set of calibration constants. A fraction of such events will be recorded to verify the proper functioning of the system and to cross-check both absolute calibration (using the Z mass constraint) and tower to tower inter-calibration. The set of calibration constants will be refreshed every few days to accomplish the task of absolute calibration and long term monitoring.

Changes in calorimeter response, inside periods of 3 to 4 days, cannot be measured with the single or double electrons as described above due to a lack of statistics. In order to follow the calorimeter response over the short term (day by day) the systems described in the section on monitoring, below, will be used. Variations detected by these systems will be recorded and used to correct the calibration constants.

6.5.2. Monitoring.

Research is needed to find the optimum techniques for monitoring the Shashlik towers and this work will form part of the Shashlik R&D program. We plan to install at least two independent light flasher systems to monitor each Shashlik tower. Light flasher systems are used on OPAL[42], L3[43], Crystal Barrel[44] and CLEO[45]. The fully commissioned systems on these experiments appear to achieve the necessary precision that would be required for monitoring the Shashlik towers. Day to day gain changes have been monitored to a precision of 0.2%.

Up to four optical fibers will be inserted into each Shashlik tower in order to monitor the performance of the scintillator plates and the wavelength shifting fibers. One or two fibers will run the full length of each tower and will be used to pass light to all scintillator layers. A further one or two fibers will be used to pass light to a few planes of scintillator near the shower maximum, in order to evaluate the effects of radiation damage. The radiation damage may cause a loss in light yield from the scintillator plates or a loss of efficiency or an increase in attenuation in the WLS fibers.

a) Monitoring by scintillator excitation .

We intend to flash light from xenon flash lamps or excited liquid scintillator (using UV lasers), to some of the optical fibers in each tower in order to excite the scintillator plates. The system will pulse many towers at the same time and will be monitored by a photodiode. Such a system will provide relative inter tower calibration.

The pulse to pulse fluctuations of the intensity from xenon flash lamps have been measured to be around 0.45% R.M.S. from the barrel lead glass system on OPAL [47]. Filters are used on the L3 xenon calibration system in order to obtain a range of light intensities corresponding to energies from 0.23 GeV to 30 GeV [48]. This may be useful for monitoring the response of the ADC and trigger systems.

---

[42] The OPAL detector at LEP, NIM A305(1991) 275.
[43] The xenon monitor of the L3 electromagnetic calorimeter, NIM A321(1992) 119.
[44] E. Aker et al., CERN-PPE/92-126(1992)
[45] Y. Kubota et al., NIM A320 (1992) 66.

b) LED monitoring .

We intend to install a single LED for each Shashlik tower. The LED will be used to flash light into one of the optical fibers of the tower. As part of the R&D program a range of LED's, emitting at different wavelengths, will be tested. Of particular interest will be any LED's which are capable of exciting the scintillator plates of the Shashlik.

The LED system is essential for single-tower testing, commissioning and subsequent monitoring and fault finding. It enables various configurations of towers to be pulsed, which may be useful for checking the trigger system. It also acts as a backup to the xenon or liquid scintillator monitoring. It is reliable over short term periods (day to day). The overall stability of LED's, however, is not sufficiently good for this system to be used as a stand alone calibrator in its own right.

c) Photodiode monitoring .

Photodiodes, both for Shashlik readout and for the monitoring system, could be monitored with gamma sources. L3 use the photo peak produced by the 59.5 keV gamma ray line of Am^{241}. In order to match the pulse height from their xenon lamp to the one of the photo peak it was found necessary to attenuate the xenon light by a factor of one thousand using a package of Kodak filters. The use of such sources will be evaluated during the R&D program.

d) Electronics monitoring .

A precision electronic pulser system will be used to monitor and calibrate the electronics chain downstream of the photodiodes.

e) Slow control monitoring .

A number of slow control monitors will be required. These will be needed to monitor such items as detector temperature, low voltage supplies, photodiode bias voltage, and the relative clock timing of the Fermi chips if these are used for readout.

6.6. Simulation studies.

6.6.1. Introduction

The construction and test in beam of the prototype calorimeter modules and preshower detector, will be followed closely by Monte-Carlo simulations. This will allow a better insight and understanding of the test results. Once tuned with respect to the test data, the simulation tools will be used to optimize the detector parameters and to study the sensitivity to the tolerances on these parameters. The effect of radiation damage on the calorimeter performance must be also modeled.

The simulation study of the Shashlik calorimeter and preshower detector was started about one year ago within the CMS collaboration. A detailed description of the work done so far can be found in references 46, 47, 48, 49. Here we want to introduce briefly the existing simulation tools and the results already obtained.

6.6.2. Energy resolution study.

The estimation of the energy resolution, linearity and uniformity of the calorimeter modules, as well as the angular resolution and π^0/γ separation in several preshower and split module configurations was done using GEANT 3.15. The program contains a detailed description of the geometry, following the design of the prototype modules, and includes a description of the light collection efficiency in each fibre. Other effects such as the attenuation in the fibres, the reflection at the fibres front face, and the photoelectron statistics were included as well. The simulation was tuned by comparing with the results obtained by other groups using the same calorimeter technique[50,51]. Up to now only non-projective geometries were simulated.

The energy resolution of the standard non-projective Shashlik module was found to be $\sigma/E=8.5\%/\sqrt{E}\oplus 1\%$ in excellent agreement with the test beam results[47](Figure 29). The study of the calorimeter response as a function of the impact point indicates a reduction of the signal of the order of 2-3% near the edges of the modules [49] (see Figure 30).

The sensitivity of the energy resolution to the optical parameters of the calorimeter was checked, in particular the effect on the constant term of the fibre attenuation length and of the reflectivity at the aluminized end. No significant variations were observed for values of the attenuation length down to λ_a = 100 cm, as well as for values of the reflectivity down to 0.5[49] No significant degradation of the energy resolution was observed when a 10% R.M.S dispersion, in the optical characteristics of the fibres and scintillator plates[47] was introduced.

The effect of the radiation damage on the energy resolution was estimated considering that the calorimeter receives a dose that follows the longitudinal profile of typical showers in minimum

[46] CMS TN / 92-45.
[47] CMS TN / 93-66.
[48] CMS TN / 93-65.
[49] CMS TN / 93-71..
[50] B.Loehr et al., NIM A254 (1987) 26.
[51] G.S.Atoyan et al., Preprint INR - 736 / 91, 1991.

bias events (E=1-3 GeV). One assumes further that the scintillator light yield and the fibres attenuation length degrades linearly with the dose. In order not to increase too much the constant term the reduction of the light yield should not exceed 10% [47] (see Figure 31).

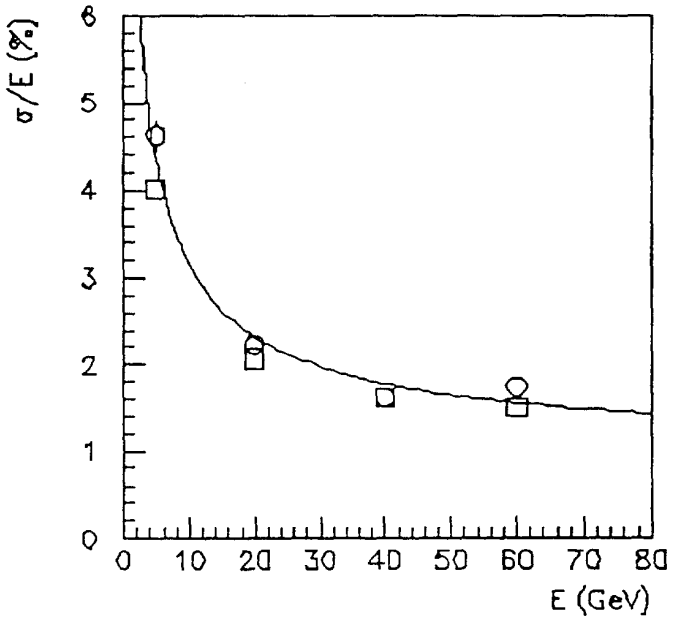

Figure 29 - Energy resolution as a function of the electron energy: without preshower (squares) and with preshower (circles). The curve corresponds to a fit to the resolution points with preshower.

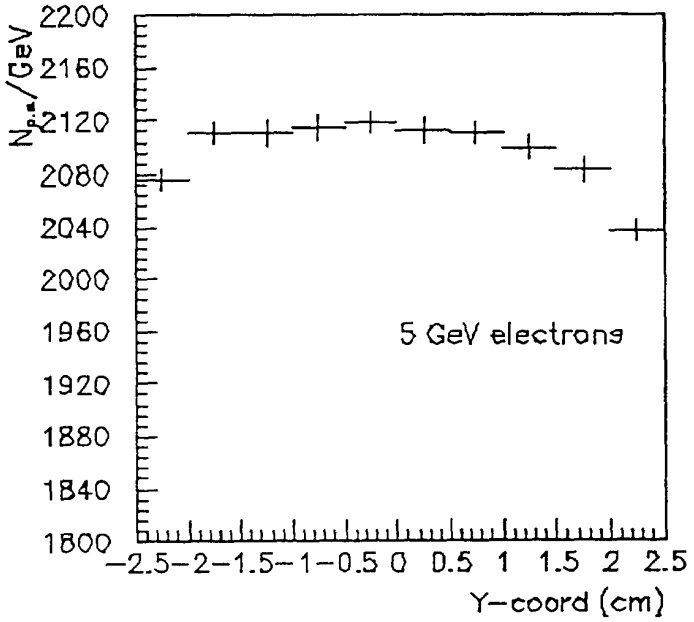

Figure 30 - Response as a function of the Y-coordinate of the impact point.

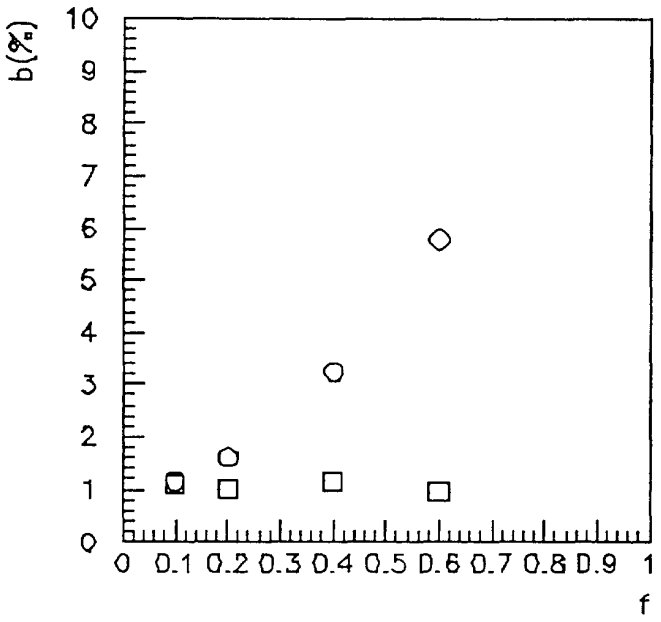

Figure 31 - Constant term of the energy resolution function versus the fractional light loss in the scintillator plate at the position of maximum damage (circles); and as a function of the fractional reduction of the fiber attenuation length at the position of maximum radiation damage (squares).

6.6.3. Angular resolution studies.

In order to assess the Shashlik angular resolution and two shower separation capabilities, three different detector configurations were studied[52]:

• Shashlik modules divided in two longitudinal segments (first segment $4X_0$), with two layers of orthogonal Si strips in between.

• Shashlik modules, front face 4x4 cm^2, combined with a preshower detector with the following structure: 2 X_0 Pb absorber- Si ϕ-strips (4 mm) - 1X_0 Pb absorber - Si η-strips (2 mm) ;

The configuration with the preshower detector gives the best results on the angular resolution and π_0/γ separation. We get σ_θ = 9.5 mrad at E_γ = 60 GeV compatible with the measurements performed in beam with a 4.5X_0 Pb absorber placed in front of the calorimeter modules[49].

[52] CMS Technical Note in preparation

a) Effect of Preshower on energy resolution.

The energy resolution of the Shashlik-preshower configuration was estimated, after correction of the calorimeter energy using the information provided by the preshower Si-strips. The result is $\sigma/E=9.4\%/\sqrt{E}\oplus 1.\%$, showing that the degradation in the energy resolution induced by the preshower is expected to be small (Figure 31).

b)Results from fast simulation.

Detailed shower simulations based on the GEANT package are very expensive in terms of CPU time. To overcome this limitation, a fast Monte-Carlo simulation was developed[53], based on a parametrization of the longitudinal and transverse profile of the showers as a function of the energy. The transverse shower shape is found to be in excellent agreement with the DATA as illustrated on figure 32.

An exploratory study of the position and angular resolution with the Shashlik calorimeter using the fast simulation was made [37]. In particular, the greater flexibility of the fast simulation allowed a detailed investigation, with high statistics, of the dependence of the position and angular resolution on transverse size and longitudinal segmentation of the calorimeter modules .

c) Uniformity of light collection.

The light collection system of the Shashlik calorimeter, based on a matrix of WLS fibers, is potentially a source of non-uniformity which can degrade the calorimeter uniformity and energy resolution (especially the constant term). A good understanding of the optical behavior of the system is needed to determine the geometrical and optical parameters that maximize the uniformity of the light yield. A dedicated Monte Carlo simulation was done to compute the efficiency of light collection as a function of the point in the scintillator plate where the light is produced. A large number of rays generated in random direction are followed until they hit a hole surface at an angle smaller than the total reflection angle or until they are lost at the surface of the plate or are absorbed inside it; the efficiency is given by the ratio between the number of rays going through a hole surface and being absorbed in the fiber, and the total number of generated rays.

[53] CMS TN / 93-63.

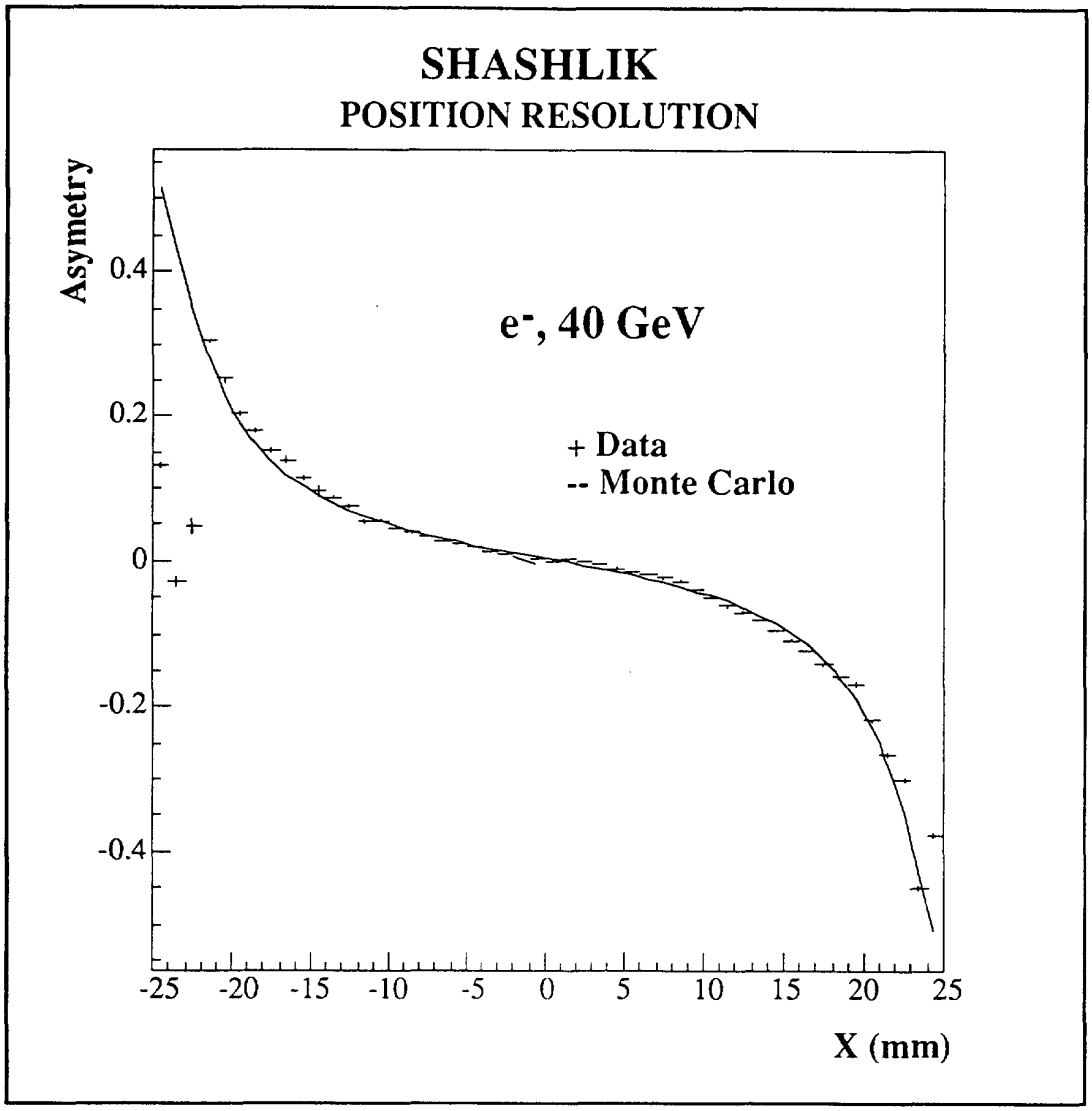

Figure 32: Measured asymmetry for all 40 GeV electron data hitting the central tower of our experimental setup (see figure 3) and Monte Carlo prediction.

6.6.4. Simulation R&D goals.

We turn now to the future simulation developments to be carried out in the context of the present proposal. Our activity will be organized in three complementary directions:

- improvement of the simulation tools;
- extensive comparison with the test data;
- optimization of the detector parameters.

The GEANT simulation programs will be upgraded in order to precisely describe the details of the Shashlik and preshower prototypes (materials, electronic noise, light collection, etc.). In particular the simulation of the projective geometry must be implemented. In order to be able to reproduce with good accuracy the non-uniformity due to the fibers, the light collection parametrization will be integrated in the fast simulation program.

These simulation tools will allow extensive comparisons with the test beam data collected, in terms of the energy resolution, uniformity and position and angular resolution. The efficiency of the light collection system as a function of its parameters (number and diameter of the fibers, reflectivity at the scintillator plate surfaces, etc.) will be simulated and compared to the results of real measurements. The following aspects will be studied:

- geometrical parameters of the preshower detector (absorber structure and thickness, silicon strips width and thickness, etc.)
- geometrical parameters of the Shashlik modules (module dimensions, sampling, productivity, etc.)
- geometrical integration of the preshower and calorimeter
- effect of dead materials
- effect of magnetic field
- optical and geometrical parameters of the light collection system (number and diameter of the fibers, attenuation lengths, reflectivity's, etc.)
- dependence on the tolerances of the geometrical and optical parameters
- effect of radiation damage.

6.7. Shashlik radiation hardness[54].

6.7.1. Introduction.

The use of plastic scintillator based calorimeters at the LHC requires good radiation tolerance. The dose at shower maximum in the barrel will be smaller than 1 kGy per year. It will reach 6 kGy per year in the end-cap. The most serious consequence of damage is the loss in the light yield. A drop of 10 % to 20 % at shower maximum is acceptable, assuming a good calibration procedure.

6.7.2. Definition of the radiation hardness coefficients.

Many data concerning radiation damage are presently available. The systematic comparison is not easy and it is convenient to define some coefficients, in order to quantify the radiation resistance of a Shashlik module. One has to consider separately the plastic scintillating plates (SCI) and the wave length shifting fibres (WLS). One defines two coefficients: (γ_{SCI}, α_{SCI}) for the scintillator and (γ_{WLS},α_{WLS}) for the WLS fibres.

The **light yield** variation in the scintillator tiles is given by the γ_{SCI} coefficient. For a given excitation, the local light emission I(Dose) is given by:

$$I(Dose) = I(0) \exp(-Dose / \gamma_{SCI})$$

where I(0) is the light emission before irradiation.

The local variation of the **attenuation length** (λ(Dose)) is described by the α_{SCI} coefficient:

$$1/\lambda(Dose) = 1/\lambda(0) + Dose\ \alpha_{SCI}$$

where $\lambda(0)$ is the attenuation length before irradiation.

In the same way, the conversion efficiency and the attenuation length (λ) of the WLS fibres can be described by the coefficients γ_{WLS} and α_{WLS}.

In a Shashlik module one has two parameters. The first one γ concerns the light yield at a given depth. The second one α is related to the attenuation length.

For the injection moulded scintillators using granulated polystyrene and K27 doped WLS fibres, we estimate:

γ	110 kGy
α	.0004 kGy^{-1} cm^{-1}

[54] J. Badier. Shashlik radiation hardness. CMS TN / 93-97.

Using these coefficients and folding in the longitudinal damage profile we can estimate the loss in light due to decreased attenuation length and light yield. These and the induced constant term are shown in figure 33. Using presently available materials, it appears that the Shashlik calorimeter can tolerate an integrated dose over 10 years at the nominal LHC luminosity (10^6 pb^{-1}) up to $|\eta| = 2$.

6.7.3. Natural aging.

Another point of concern is the natural aging of the scintillator based systems. We plan to have several modules which will be periodically tested in beam to monitor the light yield.

6.7.4. Radiation hardness R&D goals.

The first aim is a search for an optimal SCI-WLS combination and for the best fabrication methods. Investigation of the radiation hardness with low dose rates, neutron irradiation and hadron irradiation will be necessary .

Systematic irradiation has to be carried out on various types scintillating tiles and WLS fibres. For each type, a sufficient number of samples have to be measured.

The respective qualities of K27 and Y7 WLS fibres have to be compared.

Optimized SCI-WLS combination have to be used, in order to measure experimentally the γ and α Shashlik coefficients. Full size detector modules have to be therefore irradiated.

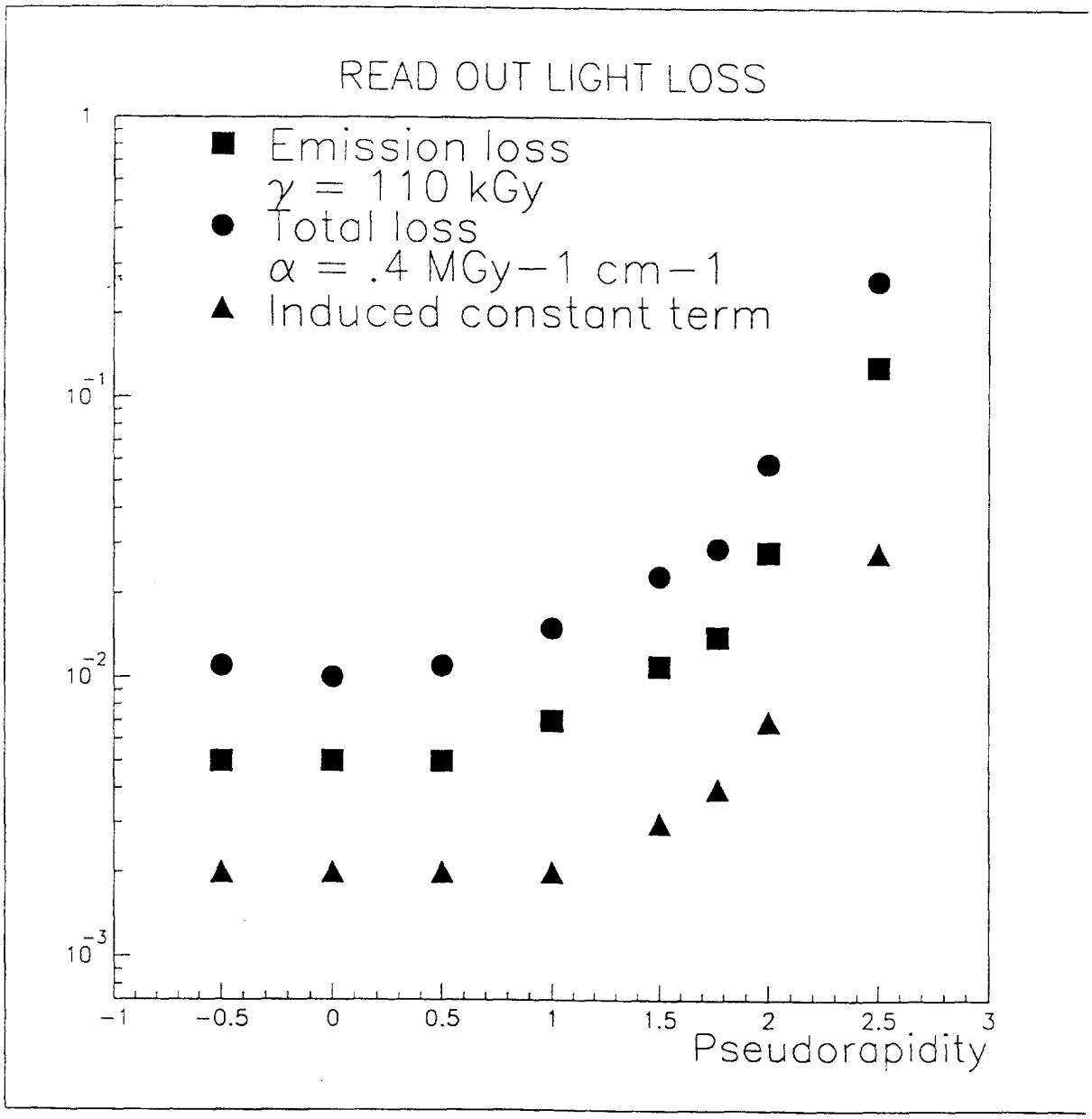

Figure 33. Losses of light and resolution degradation as a function of the pseudorapidity in the CMS-ECAL for an integrated luminosity of 10^{42} cm^{-2} and an absorption cross section of 60 mb.

6.7.5. Facilities for the radiation hardness studies.

Inside the collaboration there exist various facilities for irradiation tests. Table 7 gives the summary of these facilities as well as the type of irradiation which could be performed and the type of studies which could be undertaken.

Facility	Type of irradiation	Type of study
INR and Protvino	Strong cobalt source	Radiation hardness of: scintillator, WLS fibres, electronic components
LiL at CERN	High intensity electron beam[55]	Radiation hardness of: all type of materials, Shashlik towers.
Brunel	strong γ source[56] Pulsed 4 MeV LINAC	Radiation hardness of: scintillator, WLS fibres, electronic components
BNL[57]	High intensity π beams[58]	Radiation hardness of: Shashlik towers irradiated with π and neutrons.
Saclay	cobalt source	Radiation hardness of: scintillator, WLS fibres, electronic components
Saclay	neutron source	Radiation hardness of: mechanical assembly, glued pieces, scintillator, WLS fibres, electronic components

Table 7: Irradiation facilities: type of irradiation which could be performed and the type of studies which could be undertaken.

[55] The beam energy is ~500 MeV. The intensity can be varied from 10^9 to few 10^{10}. In 1 hour, with 2 10^9 electrons, one can produce a dose of ~6 Mrads at the shower maximum in a Shashlik tower.
[56] 4 Ci Co^{60} and 500 Ci Co^{60}.
[57] Under the responsibility of INR who has a wall of 1000 Shashlik towers in an experimental beam. They can put at the beam dump position some towers, irradiate them with 7 GeV π. The π intensity is 10^9 π /burst. After the irradiation they can follow the change of the response with minimum ionizing particles.
[58] Reproduce to some extends the working conditions at LHC.

7. Beam test requirements.

In 1993, new sets of Shashlik towers were constructed:

• Five parallelipedical towers (using the gluing technique described in section 6.1) for radiation hardness tests,

• Sixteen projective towers in η and Φ,

All have been studied in the CERN SPS H2 beam in May 1993. About 10^6 electron triggers have been taken at energies between 10 and 150 GeV. Part of the data have been taken with two planes of silicon detectors[59] in front of the calorimeter.

Two other test beam periods have been allocated for Shashlik calorimetry in 1993: one in August (3 days) and another one in October (5 days). The first one will be mainly devoted:

• to study the effect of irradiation[60] on the five towers mentioned above,

• to get more data with the 16 projective towers including the silicon preshower in front,

• to made extensive studies of uniformity of response with tilted towers,

• to test the first version of a new hybrid preamplifier designed at INR.

The last test beam period for 1993 will partly be devoted to the study of our prototypes placed in the EHS magnet. All the towers will be equipped with SiPD readout followed by the hybrid amplifiers designed at INR. The towers will have a new preshower prototype (four times larger[61] in size) covering 4 Shashlik towers. This test will mainly study the effect of the magnetic field on:

• energy resolution,

• uniformity of the response,

• position and angular resolution.

For 1994, we will prepare a new set of projective Shashlik towers with the baseline dimensions. These towers will be constructed with the techniques described in section 6.1. We have chosen to construct them in the pseudorapidity region of $\eta = 0.75$. As already mentioned, we expect to have a few such towers (9 to 16) before May 1994 and to enlarge the sample to get a matrix of 12 x 6 towers.

In parallel, developments on the preshower will continue and new prototypes will be tested in beam at the same time as the calorimeter prototypes. Work carried out in RD35 may be of direct relevance as far as Si is concerned.

In 1994, we would need about 2 months of test beam time. We will need electrons, pions and muons up to 150 GeV. The H2 beam or another beam in North area would be suitable. We wish to have the allocated beam time spread over the whole year.

[59] Size: 6 x 6 cm^2, strip width: 2 mm.
[60] These towers were irradiated at LIL up to about 3 Mrads.
[61] Size: 12 x 12 cm^2, strip width: 2 mm.

Over a longer term, final detector elements will be constructed. They will need to be calibrated in the test beam. A model of our needs is given in table 8.

	Tests			Production			Calibration	
Year	94	95	96	97	98	99	00	01
Number of days	50	100	100	50	50	200	200	200

Table 8: Required test beam time in a high energy electron and pion beam.

The beam should provide particles with momenta from 10 to 250 GeV. Some tests will be performed in magnetic field. The use of the 3 Tesla EHS magnet is essential. The test beam has also to be the same as the one for the studies of the CMS HCAL. The final calibration will be performed at 50 GeV for which a $\Delta p/p$ of 0.1% will be required. Hence equipping a new beam line may be advisable.

In parallel, we also need to perform studies related to the calorimeter response to jets which usually include low energy particles. Therefore we will need a low momentum π/K/p PS beam. The requested beam time at PS is summarized in table 9.

	Tests			Production			Calibration	
Year		95	96	97	98	99	00	01
Number of days		50	50	50	50	100	100	100

Table 9: Required test beam time at PS..

8. Sharing of responsibilities

The activities of the present R&D are the common responsibility of all institutions each of them taking part of the whole work which is shared as given in the table 10.

Institution	Shashlik Calorimeter	Preshower	Radiation	Simulation
Brunel			• Irradiation • radiation tests	
DUBNA		• Si det. production • Mec. for prototypes • Test beam DAQ	• n irradiation • radiation tests	• Simulation: - Shashlik - Preshower
CERN	• Finite element • Test beam DAQ • Readout	• Structure design • Mec. for prototypes • Readout electronic	• Irradiation at LiL	
Ecole Poly-technique	• Calo. design • prototypes • Readout	• Test beam DAQ	• Irradiation. • Data analysis	• Fast algorithms
IHEP (Protvino)	• Production of: - scintillator - WLS fibres • construction: - scint. mold – towers • Readout: - new detectors - low noise amplifiers		• Irradiation • Analysis of data	• light collection optimization
INR (Moscow)	• Production of: - scintillator - WLS fibres • construction: - scint. mold – towers • Readout: - new detectors - low noise amplifier • Monitoring	• Monte Carlo	• Irradiation • Analysis of data	• light collection optimization
Imperial College	• Finite elements • Calo. design • Readout: - photodiodes	• Test beam DAQ		
IPN Lyon	• Readout: - photodiodes - amplifiers			
ITEP	• Readout: - photodiodes			
LIP Lisboa				• Simulation: - Shashlik - Preshower
Rutherford Laboratory	• Finite elements • Calo. design • Readout: - photodiodes - amplifiers			

Table 10: Shashlik calorimetry activity sharing between the institutions involved in the R&D.

9. Request of resources and Funding.

Item	Cost (kSF)
Finished Scintillator Plates	100 K
Finished WLS fibres	20 K
Tower Assembly	in house
Tooling for towers	100 K
Tooling for quality control	100 K
Readout :	
Light detectors	100 K
Preamplifiers	100 K
Radiation studies	in house
Calibration and Monitoring	100 K
Test beam(new line) Trigger + DAQ (+ existing)	200 K
Operating costs	150 K
Preshower:	
Si	100 K
Test bench + electronics	250 K
Mechanics	100 K
Engineering studies:	
overall structure	200 K
Total	1620 K

Table 11: Requested resources for the R&D project.

We request a contribution of 30% from CERN i.e. 250 kSFr per year for the period 1994 and 1995. The remainder will be found within the rest of the collaboration.

10. R&D milestones.

The three following tables (12, 13 and 14) give the main phases and the time scale at which various steps are envisaged.

Shashlik calorimeter		
	Goals	**Milestones**
Phase 1	**Individual towers** (nonet [SiPD readout] + 16 pointing towers [PM]): • energy resolution, • shower position measurements, • uniformity of the response • response with a 3º tilt	--> August 93
Phase 2	**Individual towers in** $\vec{B}$ (16 pointing towers (52 x 52 cm^2) with [SiPD readout]): • energy resolution, • shower position measurements, • uniformity of the response • Test of readout	-> mid 1994
Phase 3	**Final size tower** in $\vec{B}$: (16 pointing towers [SiPD readout]): • energy resolution, • shower position measurements, • uniformity of the response • Test of readout	--> mid 1995
Phase 4	Large scale prototype (12 x 6 towers in $\vec{B}$ [SiPD readout]. • Test of final readout	--> end 1994

Table 12: Shashlik calorimeter R&D phases and time scale.

Shashlik preshower		
	Goals	Milestones
Phase 1	**First prototype** (2 Si planes [6 x 6 cm^2]) • effect on energy resolution, • shower position measurements, • effect on uniformity of the response	--> August 93
Phase 2	**Individual towers in $\vec{B}$ (16 pointing towers [SiPD readout] + 2 Si planes [12 x 12 cm^2])** : • effect on energy resolution, • shower position measurements, • effect on uniformity of the response • Test of readout	- -> mid 1994
Phase 3	**Final tower in $\vec{B}$: (16 pointing towers [SiPD readout]+ 2 Si planes [12 x 12 cm^2])** : • energy resolution, • shower position measurements, • uniformity of the response • Test of readout	--> mid 1994
Phase 4	**Large scale prototype (12 x 6 towers in $\vec{B}$ [SiPD readout] + large scale final geometry preshower).** • Test of final readout	--> mid 1995

Table 13 Shashlik preshower R&D phases and time scale.

Mechanical design of the calorimeter and preshower.		
	Goals	Milestones
Phase 1	Mechanical Prototypes to define the construction procedures and measure the mechanical parameters needed for finite element calculations.	--> End 93
Phase 1'	Mechanical Prototypes of the preshower detector to define the construction procedures and prepare the final mechanical design of the detector.	--> End 93
Phase 2	Finite element calculation for a barrel electromagnetic calorimeter for the glued and pocket solution. Finite element calculation for the preshower.	--> mid 1994
Phase 3	Full design of the barrel calorimeter including the preshower and definition of the construction tooling.	--> mid 1995

Table 14: Mechanical design of Shashlik calorimeter and preshower R&D phases and time scale.

11. Computing time.

From the R&D program described in this paper computing time will be required for the following:

• Each test beam period will provide us with a large amount of raw data. Our present procedure consists of first processing the data on CERN computers. This represents about 50 hours (CERN units) per 24 hours data taking. So for 1993, we will spend about 800 hours of CPU at CERN for the data processing. For 1994, our request will be of the order of 2000 hours.

• The data analysis work is performed in the different laboratories. As an example for the October 1992 data (36 hours beam time), Ecole Polytechnique carried out the bulk of the analysis and used 1000 hours CPU time. An extrapolation of this to 1993 will represent about 2000 hours, and in 1994 about 3000 hours.

• Finally, to understand the data, we have to perform extensive GEANT simulations. Detailed simulation is time consuming. For this reason we have developed a fast simulation algorithm for the electromagnetic shower development in the calorimeter. Even then a large amount of CPU is required. Our request for 1993 is 2500 hours and 5000 hours for 1994.

• CAD design on Work Stations using EUCLID or similar programs. Several groups in the collaboration are equipped with this facility. However, some of them will need to increase the computing power.

• Finite element calculations. The mechanical structure we propose for the electromagnetic calorimeter of CMS is a high precision object. It is obvious that we will need to check the designs before the final construction starts. Mechanical prototypes are needed to obtain the mechanical parameters to be inserted into the finite element programs. Several hundreds of hours of CPU time will be needed at CERN and outside to perform these calculations.

12. Conclusions.

New techniques have been developed to read out the light from lead/scintillator sampling calorimeters. These techniques involve the use of wavelength shifting optical fibres. The light yields from such calorimeters are in excess of 10000 photons per GeV. The use of optical fibres enables fine lateral segmentation to be achieved with a minimum of dead space. In addition, it is expected that such calorimeters can be built at a relatively low cost. The first results, from a non-projective calorimeter prototype exposed to high energy electrons, are encouraging. The measured energy resolution is:

$$\frac{\sigma}{E} = \frac{(8.4\pm.1)}{\sqrt{E}} \oplus \frac{(.37\pm.03)}{E} \oplus (.8\pm.2) \quad \% \quad (E \text{ in } GeV)$$

The angular resolution deduced from measurements is:

$$\sigma_\theta(\text{mrad}) = \frac{70}{\sqrt{E}}$$

The performance is good enough to observe (5σ) the Standard Model $H\rightarrow\gamma\gamma$ in the mass range ($90 < m_H < 130$ GeV) after one year of LHC running at high luminosity.

Further R&D work is essential before building a full scale projective detector. Amongst the large number items requiring R&D, we list below the items of highest priority:

- Demonstrate that for a pointing geometry one can achieve a good uniformity response. Special care has to be given to tower edges as well as to the tower to tower boundaries.
- Find the best scintillator/WLS fibre combination that provides high light output and can tolerate the LHC high radiation level without worsening too much the constant term in the energy resolution function.
- Demonstrate that one can find a Preshower + Shashlik calorimeter geometry which gives the required angular precision and π^0 rejection whilst maintaining good energy resolution and uniformity of the electromagnetic calorimeter.
- Design and build a cheap, low noise, radiation resistant readout electronics for the calorimeter and for the preshower.
- Make the mechanical tests of the gluing technique proposed for the tower construction, and the full detector. In parallel, an alternative solution for the mechanical structure will also be developed.
- Work in high magnetic field to study its effect on the calorimeter response.
- An extensive Monte Carlo simulation programme.
- calibration and monitoring,
- radiation resistance of all components of the detectors,
- investigate alternative photo-detectors,
- quality control and the acceptable limits for the large scale production of the components.

To achieve the program we have defined in this paper, we will need two years with intermediate milestones as defined in section 10.